

RESEARCH ARTICLE

SP-R210 (Myo18A) Isoforms as Intrinsic Modulators of Macrophage Priming and Activation

Linlin Yang^{1,8}, Marykate Carrillo^{1,8}, Yuchieh M. Wu^{1,8}, Susan L. DiAngelo^{1,7}, Patricia Silveyra^{1,3,7,8}, Todd M. Umstead^{1,7}, E. Scott Halstead^{1,6,8}, Michael L. Davies^{1,8}, Sanmei Hu^{1,8}, Joanna Floros^{1,4,7}, Francis X. McCormack¹⁰, Neil D. Christensen^{2,5,9}, Zissis C. Chroneos^{1,2,8*}

1 Department of Pediatrics, Pennsylvania State University College of Medicine, Hershey, Pennsylvania, United States of America, **2** Department of Microbiology and Immunology, Pennsylvania State University College of Medicine, Hershey, Pennsylvania, United States of America, **3** Department of Biochemistry and Molecular Biology, Pennsylvania State University College of Medicine, Hershey, Pennsylvania, United States of America, **4** Department of Obstetrics and Gynecology, Pennsylvania State University College of Medicine, Hershey, Pennsylvania, United States of America, **5** Department of Pathology, Pennsylvania State University College of Medicine, Hershey, Pennsylvania, United States of America, **6** Division of Pediatric Critical Care Penn State Hershey Children's Hospital, Pennsylvania State University College of Medicine, Hershey, Pennsylvania, United States of America, **7** Center of Host Defense and Lung Disease Research, Pennsylvania State University College of Medicine, Hershey, Pennsylvania, United States of America, **8** Pulmonary Immunology and Physiology Laboratory, Pennsylvania State University College of Medicine, Hershey, Pennsylvania, United States of America, **9** The Jake Gittlen Laboratories for Cancer Research, Pennsylvania State University College of Medicine, Hershey, Pennsylvania, United States of America, **10** Department of Internal Medicine, Division of Pulmonary, Critical Care and Sleep Medicine, University of Cincinnati College of Medicine, Cincinnati, Ohio, United States of America

These authors contributed equally to this work.

* zchroneos@hmc.psu.edu

Abstract

The surfactant protein (SP-A) receptor SP-R210 has been shown to increase phagocytosis of SP-A-bound pathogens and to modulate cytokine secretion by immune cells. SP-A plays an important role in pulmonary immunity by enhancing opsonization and clearance of pathogens and by modulating macrophage inflammatory responses. Alternative splicing of the *Myo18A* gene results in two isoforms: SP-R210_S and SP-R210_L, with the latter predominantly expressed in alveolar macrophages. In this study we show that SP-A is required for optimal expression of SP-R210_L on alveolar macrophages. Interestingly, pre-treatment with SP-A prepared by different methods either enhances or suppresses responsiveness to LPS, possibly due to differential co-isolation of SP-B or other proteins. We also report that dominant negative disruption of SP-R210_L augments expression of receptors including SR-A, CD14, and CD36, and enhances macrophages' inflammatory response to TLR stimulation. Finally, because SP-A is known to modulate CD14, we used a variety of techniques to investigate how SP-R210 mediates the effect of SP-A on CD14. These studies revealed a novel physical association between SP-R210_S, CD14, and SR-A leading to an enhanced response to LPS, and found that SP-R210_L and SP-R210_S regulate internalization of CD14 via distinct macropinocytosis-like mechanisms. Together, our findings support a model in



OPEN ACCESS

Citation: Yang L, Carrillo M, Wu YM, DiAngelo SL, Silveyra P, Umstead TM, et al. (2015) SP-R210 (Myo18A) Isoforms as Intrinsic Modulators of Macrophage Priming and Activation. PLoS ONE 10(5): e0126576. doi:10.1371/journal.pone.0126576

Academic Editor: Martin E Rottenberg, Karolinska Institutet, SWEDEN

Received: September 10, 2013

Accepted: April 6, 2015

Published: May 12, 2015

Copyright: © 2015 Yang et al. This is an open access article distributed under the terms of the [Creative Commons Attribution License](https://creativecommons.org/licenses/by/4.0/), which permits unrestricted use, distribution, and reproduction in any medium, provided the original author and source are credited.

Funding: This work was supported in part by National Institutes of Health grants HL-34788 and HL068127, and the Children's Miracle Network. The funders had no role in study design, data collection and analysis, decision to publish, or preparation of the manuscript.

Competing Interests: The authors have declared that no competing interests exist.

which SP-R210 isoforms differentially regulate trafficking, expression, and activation of innate immune receptors on macrophages.

Introduction

The surfactant protein A (SP-A) receptor 210 (SP-R210) is a product of the unconventional *Myosin 18A* (*Myo18A*) gene, also known as MysPDZ [1–4], MyoXVIII A [2, 5, 6], or Myosin-18 [7]. The *Myo18A* gene encodes two SP-R210 splice isoforms in macrophages, namely SP-R210_L and SP-R210_S [8], also known as MysPDZ α or Myo18A α and MysPDZ β or Myo18A β [1, 9, 10], respectively. In macrophages, SP-R210 mediates phagocytic and immuno-regulatory functions of SP-A [5, 8, 11–17]. The larger SP-R210_L or Myo18A α isoforms are distinguished from the short SP-R210_S or Myo18A β isoforms by an amino-terminal extension containing a PDZ domain [3, 5]. In the present report, we use the acronym SP-R210 and Myo18A for immune and non-immune cells, respectively. The reason for this name nomenclature is based on experimental and computational evidence indicating that the *Myo18A* gene is subject to cell type-dependent alternative splicing. For example, in addition to splicing that generates SP-R210_L and SP-R210_S isoforms, splicing of small exons generates alternate forms of the unique carboxy-terminal domain of Myo18A in macrophages [6]. Moreover, recent work presented in abstract form suggested that alternate splicing introduces new motifs affecting localization of Myo18A α to dendritic spines of Purkinje neurons (<http://researchfestival.nih.gov/2011/posters.cgi?id=CELLBIO-1>).

Even though Myo18A belongs to the myosin family, it is not a typical mechano-enzyme as indicated by lack of ATP hydrolysis that normally couples myosin to the actin cytoskeleton [1, 7, 18]. Myo18A α , however, appears to regulate cytoskeletal network interactions in subcellular membranes through binding different protein or lipid targets in different cell types [9, 19–22]. Studies in various mammalian cells have reported that Myo18A α modulates Golgi structure [21], budding of Golgi secretory vesicles [20, 21], and retrograde flow of cell membrane lamellipodia [22, 23]. In migrating cells, Myo18A α localized to integrin adhesion complexes [19], and, in B lymphocytes, Myo18A α localized with ezrin and the B cell receptor [9], suggesting roles for Myo18A α in cell signaling processes. Interestingly, immune activation results in localization of SP-R210 on the surface of T lymphocytes [12]. On the other hand, the SP-R210_L and SP-R210_S cell-surface isoforms in macrophages assume a novel myosin function in recognition and uptake of SP-A opsonized bacteria [5, 8]. In addition to this opsonic function, studies in U937 cells, which exclusively express SP-R210_S, indicated that SP-R210_S mediates endocytosis of SP-A [24].

SP-A has been shown to either bind or stimulate a number of receptors on macrophages [11, 25]. Different studies reported that SP-A could stimulate IgG Fc and complement-dependent phagocytosis of opsonized bacteria [26, 27]. Furthermore, SP-A was shown to also stimulate expression of non-opsonic receptors and phagocytosis through the macrophage mannose [28, 29] and scavenger receptors [30, 31]. Phagocytosis of SP-A-opsonized bacteria via SP-R210 is coupled to macrophage activation state as indicated by increased production of TNF α and nitric oxide [8, 13]; disruption of SP-R210_L abrogated phagocytosis of SP-A-opsonized bacteria [8]. On the other hand, ligation of SP-R210 by free SP-A suppresses responses to inflammatory stimuli [12, 14, 24]. Binding of the SP-A collagen-like domain to the CD91/calreticulin receptor complex enhances uptake of SP-A-coated apoptotic cells and also results in pro-inflammatory responses [32]. SP-A, however, facilitates tonic suppression of alveolar macrophages under normal circumstances and helps restore resolution of inflammation by binding the immunosuppressive receptor SIRP α on alveolar macrophages [32, 33]. SIRP α suppresses downstream signaling through

activation of SHP-1 phosphatase. Furthermore, binding of SP-A to SIRP α inhibits phagocytosis of apoptotic cells by alveolar macrophages through activation of SHP-1 and RhoA [33]. The globular carbohydrate recognition domain (CRD) of SP-A is responsible for binding to SIRP α [33]. The CRD domain of SP-R210 is also responsible for binding and suppressing pro-inflammatory CD14 and TLR pattern recognition receptors. In this regard, chronic exposure of human alveolar macrophages to SP-A and surfactant lipids increase expression of IRAK-M, which acts as an antagonist of TLR signaling [34]. Binding of SP-A to CD14 [35–37] and TLR-4 [38, 39] inhibits the inflammatory response to LPS, by a mechanism that alters trafficking of TLR-4 between golgi and endosomal vesicles in response to LPS [40]. On the other hand, earlier studies showed that SP-A enhances the ability of human macrophage cell lines to generate an inflammatory response as indicated by increased levels of the membrane receptors CD14, CD54, and CD11b, and elaboration of inflammatory cytokines [41–43]. In this case, surfactant lipids inhibited the inflammatory function of SP-A. Lack of SP-A alters the proteomic profile of alveolar macrophages in mice [44]. Importantly, pulmonary administration of human SP-A isolated from normal individuals [44] or alveolar proteinosis patients [45] to SP-A-deficient mice nearly restored the proteomic profile and rescued phagocytic activity of alveolar macrophages similar to WT mice, respectively, indicating that human and mouse SP-A modify alveolar macrophage phenotype and function similarly. In preceding studies, SP-A was shown to induce cross-tolerance or priming of differentiated monocytic cell lines as indicated by inhibition or enhanced secretion of different cytokines [46, 47], although the receptors were not identified. Interestingly, recent studies indicate that TLR-2 mediates several SP-A functions in suppressing responses to multiple inflammatory agents [48], in enhancing macrophage chemotaxis [49], and in modulating the timing of parturition [48, 50]. Taken together, SP-A utilizes diverse regulatory and counter-regulatory mechanisms to modulate innate immune functions of macrophages.

Here, we studied macrophages lacking expression of the SP-R210_L isoform. Previous findings revealed that dominant negative disruption of SP-R210_L blocked opsonic phagocytosis of SP-A-coated bacteria, but also enhanced non-opsonic phagocytosis via the scavenger receptor SR-A [8]. Our present findings indicate that SP-R210_L and SP-R210_S coordinate the function and expression of innate immune receptors in macrophages.

Materials and Methods

Reagents and antibodies

Chemicals were purchased from Sigma-Aldrich (St. Louis, MO). Pre-stained molecular weight markers were from Bio-Rad (Hercules, CA), and fetal bovine serum (FBS) from Atlanta Biologicals (Atlanta, GA). The TNF α ELISA kit was from eBioscience (San Diego, CA). Smooth lipopolysaccharide (LPS) from *Escherichia coli* serotypes O111:B6 or O26:B6 were from Sigma-Aldrich. The RNAeasy midi kit was from Qiagen (Valencia, CA). The High capacity cDNA reverse transcription kit and TaqMan qRT-PCR gene expression assays were from Life Technologies/Invitrogen (Carlsbad, CA). Fluorochrome conjugated monoclonal antibodies against CD11c (N418); CD11b (M1/70); CD14 (Sa2-8); CD282 (TLR-2; mT2.7); CD284 (TLR-4; UT41); SIRP α (P84); F4/80 (BM8); Ly-6C (HK1.4); TNF α (MPX-XT22), and CD16/32 Fc block (93) were from eBioscience (San Diego, CA). The CD36 (72–1) and CD284 (TLR-4; Sa15-21) antibodies were from BioLegend (San Diego, CA). The SR-AI/MSR1 (clone: 268318) and CD87 (uPAR; clone 109801) antibodies were from R&D (Minneapolis, MN). Isotype matched controls were from eBioscience or R&D. Unconjugated goat polyclonal against mouse CD14, TLR-2, CD36, SR-AI/MSR1, and rat monoclonal anti-mouse CD11b (M1/70) were purchased from R&D. Rabbit polyclonal antibodies against human SP-A were used as described previously [51]. Antibodies to SP-B were either a kind gift of Dr. Jeffrey Whitsett (Cincinnati Children's Hospital

Medical Center, Cincinnati, OH) or purchased through Seven Hills Bioreagents (Cincinnati, OH). Brefeldin A, and fix/permealizing solution for intracellular cytokine staining were from eBioscience. Antibodies to NF κ B subunit RelA(p65), RelA(p65)^{S536}, IRAK-1, and I κ B were purchased from Cell Signaling. Secondary HRP-conjugated donkey anti-goat antibodies were from R&D. TrueBlot HRP-conjugated anti-rabbit and protein G-Sepharose IP beads were from eBioscience or GE Life Sciences. The ECL chemiluminescence kit was from Perkin Elmer (Waltham, MA). Monoclonal antibodies to SPR210 were generated by standard methods as previously described [52]. The characterization and purification of monoclonal SP-R210 antibodies will be reported elsewhere. Dynasore was obtained from SIGMA, and 5-(N-Ethyl-N-isopropyl)amiloride (EIPA) and NSC23766 were from SelleckChem through Fisher Scientific.

Mice

WT C57BL/6 mice were purchased from Jackson Labs (Bar Harbor, MN). The SP-A^{-/-} mice were bred and maintained locally either at the University Of Cincinnati College Of Medicine or at Penn State College of Medicine. Mice were maintained in microisolator ventilated cages and provided autoclaved water and food ad libitum. SR-A^{-/-} transgenic mice at the two Institutions were derived independently as described previously and backcrossed [53–55] to the C57BL/6 genetic background. All procedures were in accordance to Institutional Animal Use and Care Committees.

Isolation of Alveolar Macrophages

Alveolar macrophages were isolated by alveolar lavage using five consecutive washes of alveolar contents with 0.5 mL of PBS supplemented with 1 mM EDTA. Alveolar macrophages were collected by centrifugation and processed for Western blot analysis as described previously [56].

Purification and characterization of human SP-A

SP-A was isolated from discarded therapeutic lung lavage from alveolar proteinosis patients by modifications [57] of the traditional butanol/octylglucoside extraction method of Haagsman and colleagues [58] (Method 1) or according to detailed protocols provided by Agrawal et al [48] (Method 2). SP-A preparations were dialyzed in 5 mM Hepes, pH 7.5, and stored frozen at -80°C until use. All procedures used LPS-free water from a Millipore water purification system (Millipore RiOs 16 and Milli-Q Biocell with resistance of >18.2 M Ω). The concentration of LPS in purified SP-A was measured using the Limulus Amebocyte Lysate QCL-1000 assay (Lonza, Walkersville, MA). LPS was undetectable in SP-A purified by Method 1. The concentration of LPS in SP-A prepared using Method 2 was 20 pg/ μ g of protein. Protein purity was determined by silver-staining as previously described [59]. For mass spectrometry, SDS-PAGE gels were stained with the Invitrogen SilverQuest staining kit. Proteins co-isolating with SP-A were excised, in-gel digested with trypsin and proteins identified by MALDI mass spectrometry at Penn State College of Medicine Mass Spectrometry Facility.

Cell culture

The generation of control and SP-R210_L(DN) Raw264.7 cells was recently described by us [8]. Briefly, cells were stably transfected with pTriex-2 vector expressing the carboxy-terminal domain of SP-R210 (SP-R210_L(DN) cells [6]. Control cells were transfected with empty vector. Cells were cultured for 20–48 hrs in RPMI supplemented with 10% fetal bovine serum (FBS). Cells were cultured in 96-well dishes at a density of 50,000 cell/well or 12-well dishes at a density of 150,000–250,000 cells/well.

Flow cytometry

Control and SP-R210_L(DN) Raw264.7 cells were detached using non-enzymatic cell dissociation medium (SIGMA) and washed in PBS. After blocked in PBS, pH 7.4, supplemented with 1% goat serum, 0.5% BSA, and 5 µg/mL of Fc block at a concentration of 1×10^7 cells/ml for 1 hr on ice, cells were stained with recommended concentrations of monoclonal antibodies for 30 min on ice. For viability staining, cells were washed twice with PBS without protein or azide, and then stained with eBioscience e506 fixable viability dye for 20 min at 4°C. For intracellular cytokine staining, cells were washed once with FACS buffer (PBS containing 2% FBS, 0.02% sodium azide) and fixed with 100 µl eBioscience intracellular (IC) fixation buffer for 30 min at room temperature. Then cells were permeabilized with eBioscience permeabilization buffer, and stained with anti-mouse TNF α conjugated to phycoerythrin (PE). Events were acquired using either a BD FACS Calibur or LSR II flow cytometer (BD Pharmingen) and analyzed using FlowJo flow cytometry analysis software (Treestar, Mountain View, CA).

Endocytosis assays

Control and SP-R210_L(DN) cells were placed in 12 well plates at a density of 250,000 cells/well and cultured in RPMI/10% FBS for 20 hrs. The cells were then stimulated with 100 ng/mL or 2 µg/mL of LPS for CD14 and TLR-4 endocytosis assays, respectively, and harvested at 0, 1, 2, 3, and 4 hrs post-stimulation using cell dissociation buffer. Cells were blocked and then processed for cell surface staining with PE-Cy7-conjugated CD14 (eBioscience, clone Sa2-8) or PE-conjugated TLR4 antibody (BioLegend, clone Sa15-21) for 30 min at 4°C. To test the effect of inhibitors, cells were pretreated with 80 µM dynasore to inhibit dynamin, 40 µM EIPA to inhibit macropinocytosis, or 100 µM NSC23766 to inhibit RAC1 in normal medium 30 min prior to addition of LPS.

Generation of cell extracts and Western blot analysis

Cultured cells were washed in PBS and detached using non-enzymatic cell dissociation medium. Cell suspensions were centrifuged at 210 x g at 4°C and lysed in ice-cold complete lysis buffer (50 mM Tris-HCl, pH 8.0, 150 mM NaCl, 1% NP-40 supplemented with 1 mM MnCl₂, 10% glycerol, 1x Cell Signaling Phosphatase/Protease Inhibitor cocktail) by freeze and thaw cycles as described previously [12]. Extracts were used immediately, or stored frozen at -80°C. Proteins were separated on 4–17% SDS-PAGE gradient gels and transferred to nitrocellulose by semi-dry blotting. The blots were then blocked in Tris-buffered saline, pH 7.5, supplemented with 0.1% Tween 20, and 5% non-fat dry milk. Blots were probed with anti-Myo18A, CD14, SR-A, TLR-2, or CD36 antibodies and then incubated with of HRP-conjugated anti-rabbit or anti-goat secondary antibodies. Bound antibodies were visualized by enhanced chemiluminescence. Relative band intensity was determined by densitometry using a GS-800 Calibrated Densitometer (Bio-Rad) and Quantity One software (Bio-Rad).

Confocal microscopy

Macrophages grown on glass coverslips were stimulated with 100 ng/mL LPS for set time points, washed with PBS, fixed for 15 min with 4% paraformaldehyde, permeabilized for 10 min in 0.3% Triton X-100/ PBS, and then blocked in 10% goat serum/ PBS for 60 min at room temperature. Subsequently, the cells were stained with rabbit p65(ReLA) antibodies (1:400 dilution) and then with Cy3 conjugated anti-rabbit secondary antibodies (1:500 dilution). Coverslips were mounted on slides by using Prolong mounting medium with DAPI (Life Technologies). Confocal images of fluorescently labeled cells were acquired with a Leica AOBSP8 laser scanning

confocal microscope (Leica, Heidelberg, Germany) using a high resolution Leica 60X/1.3 Plan-Apochromat oil immersion objective at the Penn State College of Medicine Imaging Core. The laser lines used for excitation were continuous wave 405 (for DAPI) and 591 (for Cy3). These laser lines were produced by UV diode, 80 MHz white light laser (Leica AOBS SP8 module) respectively and the respective emission signals were collected sequentially using AOBS tunable filters. All images and spectral data measurement data were generated using the highly sensitive HyD detectors (with time gated option). The backscattered emission signals from the sample were delivered through the AOBS tunable filter (to remove irradiated laser), the detection pin-hole set to 1 Airy unit (to obtain optimal lateral and axial resolutions), spectral dispersion prism, and finally to the HyD detectors. The width of the slits in front of each HyD could be software adjusted so that each HyD could detect spectral regions spanning from a 10-nm bandwidth up to the overall spectral capacity of the system (400–800 nm). Using this unique option, spectral scanning was performed on all the dyes to confirm signal specificity. Confocal images were analyzed using Imaris Software.

Immunoprecipitation

Control and SP-R210_L(DN) cells were cultured in 100 mm dishes for 24 hrs and then stimulated with 100 ng/mL LPS for 10, 30, 60 and 120 minutes. After set time periods, plates were washed twice with cold PBS. Cells were lysed directly on plate using complete lysis buffer solution on ice for 30 minutes and lysates were then harvested by centrifugation for 15 minutes at 10,000 x g at 4°C. Supernatants were collected without disturbing pellets. Protein concentration of supernatants was measured by BCA Assay kit (the kit information) and 1.5–2.0 mg of protein per sample was pre-incubated with pre-equilibrated Protein G Agarose beads (Roche) on a rotator for 3h at 4°C. Beads were removed by centrifugation at 12,000 x g for 1 minute and supernatants were transferred into fresh tubes. Pre-adsorbed lysates were then incubated with indicated antibodies or isotype controls on a rotator for 1h at 4°C and then 40–50 µL of pre-equilibrated Protein G Agarose beads (1:1, beads to bed volume) were added to lysates. Samples were incubated on rotator overnight at 4°C. Immunoprecipitation products were centrifuged for 1 minute at 12,000 x g and supernatant was discarded. Beads were washed three times in lysis buffer (50 mM Tris-HCl, pH 8.0, 150 mM NaCl, 1% NP-40). After the last wash, 2x Urea sample buffer (50 mM Tris-HCl, pH 6.8, 1.6% SDS, 7% glycerol, 8M Urea, 200 mM DTT, 0.01% bromophenol blue) was added directly onto beads. Prepared samples were incubated at room temperature for 20 minutes and heated at 95°C for 2 minutes. Samples were centrifuged at 12,000 x g for 1 minute, and then separated on 4–17% SDS-PAGE gels and analyzed by Western blotting.

Quantitative real time RT-PCR

DNase-treated mRNA was isolated from control and SP-R210_L(DN) macrophages using the Qiagen RNeasy kit. cDNA was synthesized with the high capacity cDNA Reverse Transcription kit following the manufacturer's protocol. Briefly, 1 µg of purified RNA was incubated with 2 µL of 10X buffer, 0.8 µL of 25X dNTPs, 2 µL of 10X random primers, 1 µL of RNase inhibitor, and 50 U of reverse transcriptase in a final volume of 20 µL. The reaction was incubated for 10 min at 25°C, 2 hrs at 37°C, and inactivated for 5 min at 85°C. The cDNA was diluted five-fold prior to PCR amplification with TaqMan gene expression assays SR-A, CD11b, CD36, and CD14 and 18S ribosomal (r) RNA were quantified by real time RT-PCR (qRT-PCR) using TaqMan assays. SP-R210_L mRNA was measured using primers encompassing the PDZ domain containing exon 1 and exon 2 mRNA junction of the *Myo18A* gene. Common internal primers between exon 18 and 19 were used to quantify both SP-R210_L and SP-R210_S mRNA. Each 20 µL qPCR reaction included 10 µL of 2X TaqMan Gene Expression Master Mix, 1 µL of 20X

TaqMan Gene Expression Assay, and a total of 10 to 40 ng of cDNA. The reactions were incubated in 384-well optical plates at 50°C for 2 min, 95°C for 10 min, and 40 cycles of 95°C for 15 seconds and 60°C for 1 min. Each sample was analyzed in triplicate along with no-template controls. Results were monitored and stored by the ABI PRISM 7900HT sequence detection system (Applied Biosystems) at the Functional Genomics Core Facility at the Penn State College of Medicine. Expression of mRNA for each gene was normalized to 18S rRNA. Data are expressed as relative mRNA expression in SP-R210_L(DN) compared to control cells were calculated using the $2^{-\Delta\Delta Ct}$ method using the mean ΔCt in control cells as the calibrator [60].

Statistics

Statistical comparison of data was performed using GraphPad Prism 5.0 software (San Diego, CA). Pair-wise comparisons using the Wilcoxon matched pairs t test were used to assess statistical differences. $P < 0.05$ were considered significant.

Results

Dominant-negative inhibition of SP-R210_L mRNA in SP-R210_L(DN) cells

Stable expression of the unique carboxy-terminal (ct) domain of SP-R210, SP-R210ct [5, 6], in Raw264.7 macrophages resulted in selective dominant-negative (DN) inhibition of SP-R210_L [8]. SP-R210ct isoforms differ by a 15 amino acid insertion [6] designated as SP-R210_L(DN1) and SP-R210_L(DN2) on Fig 1A. Western blotting (Fig 1A) and qPCR analysis (Fig 1B) demonstrate that stable expression of either SP-R210ct deletion mutant blocked both mRNA and protein expression of SP-R210_L by more than 85%. In contrast, expression of the SP-R210_S variant did not decrease significantly.

Increased levels of innate immune receptors on the surface of SP-R210_L(DN) cells

We first asked whether disruption of SP-R210_L alters expression of innate immune receptors in addition to the previously described SR-A [8]. Studies below represent combined data from both SP-R210_L(DN) cell lines. Fig 2 demonstrates 20- and 4-fold higher cell-surface levels of the scavenger receptor class A (SR-A) and CD36 (Fig 2A), 2- to 3-fold increase in TLR-2 and CD14 (Fig 2B), and 4- and 2-fold increases in CD11b and CD11c in SP-R210_L(DN) cells (Fig 2C). Interestingly, the levels of TLR-4 were 40% lower than control in SP-R210_L(DN) cells (Fig 2B). The monocytic marker Ly-6C and uPAR were expressed at low levels and were not different between control and SP-R210_L(DN) cells (Fig 2A and 2B). The macrophage differentiation marker F4/80 was not statistically different compared to control cells (Fig 2A and 2C). Further, lack of SP-R210_L did not alter expression of SIRP α (Fig 2C). Interestingly, depletion of SP-R210_L resulted in 4- and 20-fold increases in mRNA levels of CD11b and SR-A (Fig 2D). The mRNA levels of CD14 and CD36 were similar to control cells (Fig 2D), even though surface expression of all four receptors increased significantly on SP-R210_L(DN) cells. Given that CD14 levels increased in SP-R210_L(DN) cells, we measured levels of TNF α after incubation with LPS. Control and SP-R210_L(DN) cells were treated with 100 ng/mL smooth LPS to trigger macrophage activation via CD14. Intracellular staining 4 hrs after challenge with LPS demonstrates robust increase in the synthesis of TNF α in both SP-R210_L(DN)1 and SP-R210_L(DN)2 cells compared to controls (Fig 3A). Given that similar results were obtained with SP-R210_L(DN)1 and SP-R210_L(DN)2 cells, results described in SP-R210_L(DN) are pooled data from both cell lines in subsequent studies. Fig 3B shows that SP-R210_L(DN) cells secreted significantly more TNF α compared to control cells, consistent with higher levels of CD14. Accordingly, previous studies demonstrated

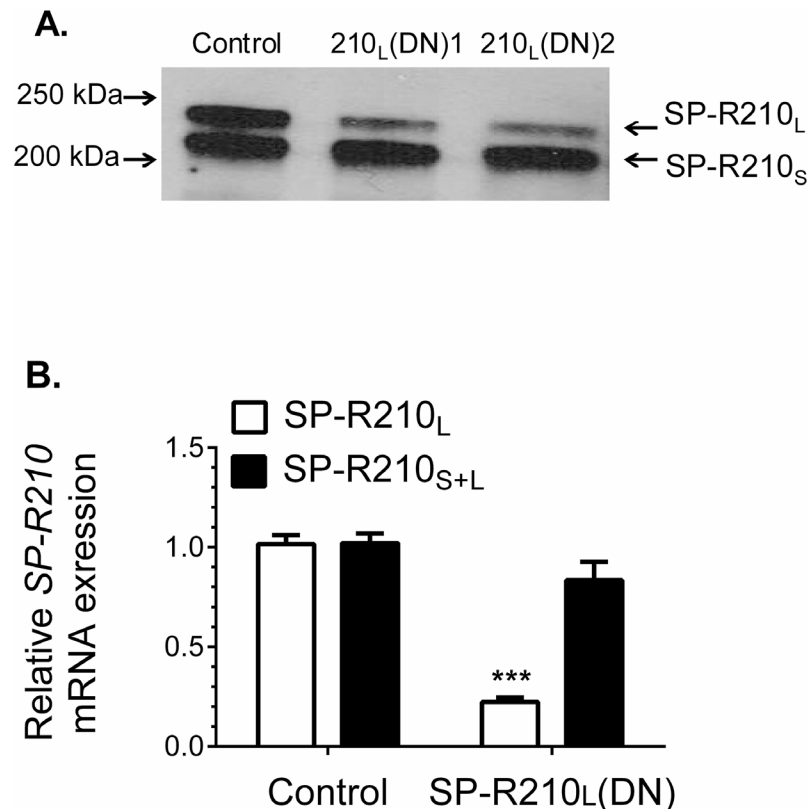


Fig 1. Dominant-negative disruption of SP-R210_L. Raw264.7 cells were stably transfected with empty pTriexNeo2 control or vector containing the 300 (210_L(DN1)) and 350 (210_L(DN2)) bp cDNA of SP-R210 carboxy-terminal isoforms (6). A) Detergent extracts were analyzed by Western blotting using affinity purified polyclonal antibodies recognizing both SP-R210_L and SP-R210_S. Lanes were loaded with 5 μg of protein. B) Total RNA from indicated cell lines was reverse transcribed and quantitated by qRT-PCR using TaqMan assays and primers encompassing the SP-R210_L-specific exons 1 and 2 (red bars) and internal primers encompassing exon 17 and 18 common to both SP-R210 isoforms (black bars) and 18S rRNA as internal control. (n = 4 ***p<0.001).

doi:10.1371/journal.pone.0126576.g001

increased functional activity of scavenger receptors [8], consistent with higher levels of SR-A and CD36 (Fig 2A) in SP-R210_L(DN) cells. Taken together, these findings indicate that SP-R210_L acts as an intrinsic repressor of innate receptor expression and function through both transcriptional and post-transcriptional mechanisms.

SP-A is a paracrine enhancer of SP-R210_L expression in alveolar macrophages

To determine whether SP-A modulates SP-R210 expression *in vivo*, SP-R210 expression was assessed on alveolar macrophages from WT and SP-A^{-/-} mice. SP-R210_L is the main isoform on alveolar macrophages (Fig 4A) consistent with previous findings [8]. Notably, alveolar macrophages from most SP-A^{-/-} mice appear to express similar levels of both SP-R210_L and SP-R210_S, suggesting differential expression of SP-R210 isoforms in the absence of SP-A *in vivo*. Densitometry analysis showed that WT macrophages express nearly five-fold higher levels of SP-R210_L compared to SP-A^{-/-} mice (Fig 4B). Similar results were obtained from the two original mouse lines maintained at the University of Cincinnati College of Medicine [61, 62] and Pennsylvania State University College of Medicine [55, 63, 64]. Consistently, treatment of

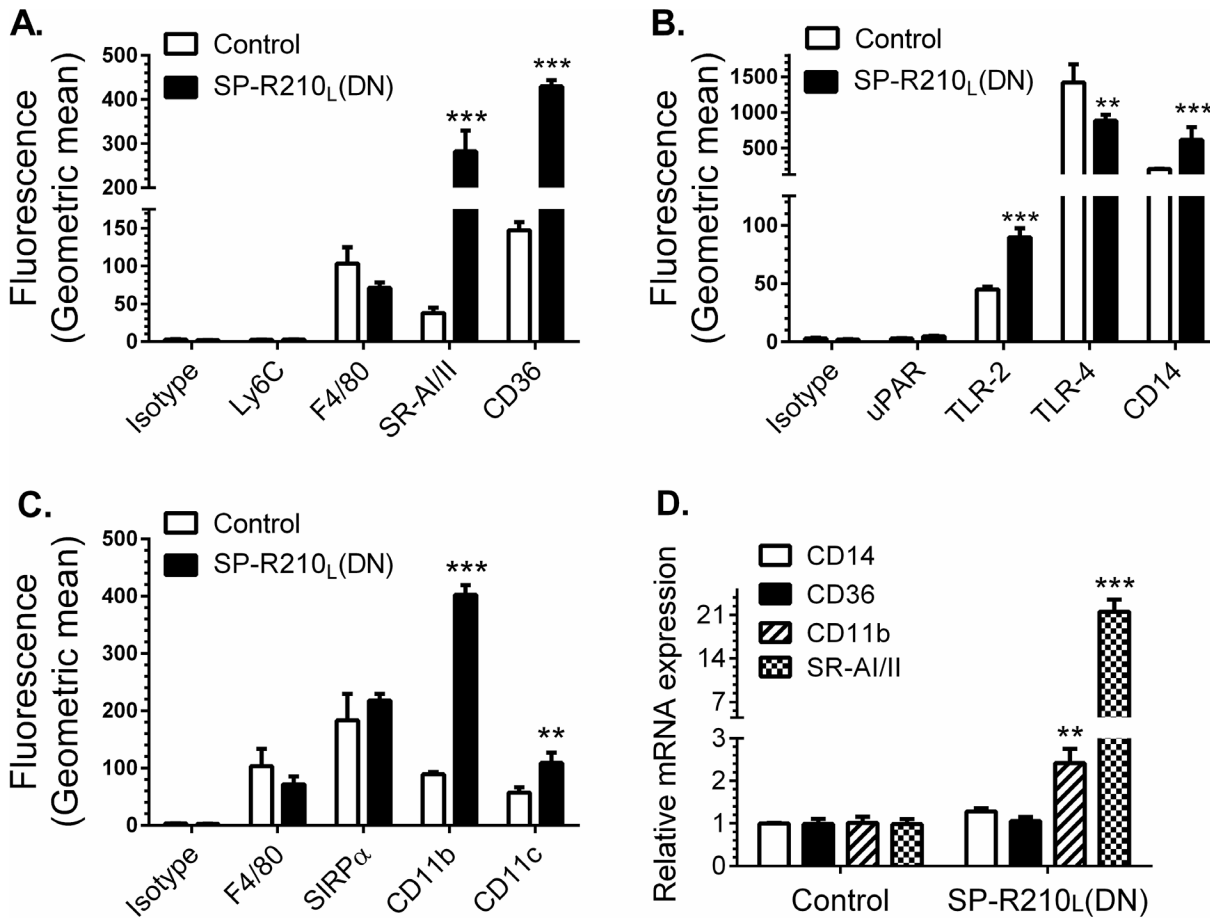


Fig 2. Depletion of SP-R210_L differentially enhances expression of innate immune receptors in macrophages. Control and SP-R210_L(DN) cells were analyzed by flow cytometry using indicated APC (A) or PE-conjugated antibodies (B, C) (n = 4–8). (D) mRNA levels of indicated receptors in SP-R210_L(DN) cells relative to control cells were determined by qRT-PCR (n = 4 independent experiments performed in duplicate, **p < 0.02, ***p < 0.005).

doi:10.1371/journal.pone.0126576.g002

Raw264.7 macrophages with SP-A *in vitro* also induced expression of SP-R210, although in this case both isoforms were induced (S1A Fig). SP-A did not induce expression of SP-R210_S in SP-R210_L(DN) cells, suggesting that SP-R210_L is required for induction of SP-R210 by SP-A (S1B Fig). Together, these results indicate that SP-A is a paracrine regulator of SP-R210 expression in macrophages.

SP-R210_S is a CD14 co-receptor

To determine whether SP-R210 modulates LPS responsiveness via CD14, we performed immuno-precipitation experiments to assess whether SP-R210 interacts physically with CD14 and used neutralizing antibodies to assess responsiveness of control and SP-R210_L(DN) macrophages to LPS. We also determined whether SP-R210 interacts with SR-A, CD11b, CD36, and TLR-2, proteins that are increased in SP-R210_L(DN) cells (Fig 2 above). Of these, CD11b, TLR-2, and SR-A were also known to interact with either SP-A [27, 48, 49] and/or SP-R210 [8]. We used an affinity purified polyclonal anti-SP-R210 antibody recognizing both SP-R210_L and SP-R210_S. Fig 5A shows that CD14 precipitated with SP-R210 antibodies in both control and SP-R210_L(DN) cells. Co-precipitated CD14 was clearly enriched in SP-R210_L(DN) cells. Interestingly, SR-A was also enriched in SP-R210_L(DN) cells, suggesting that SP-R210_L controls the

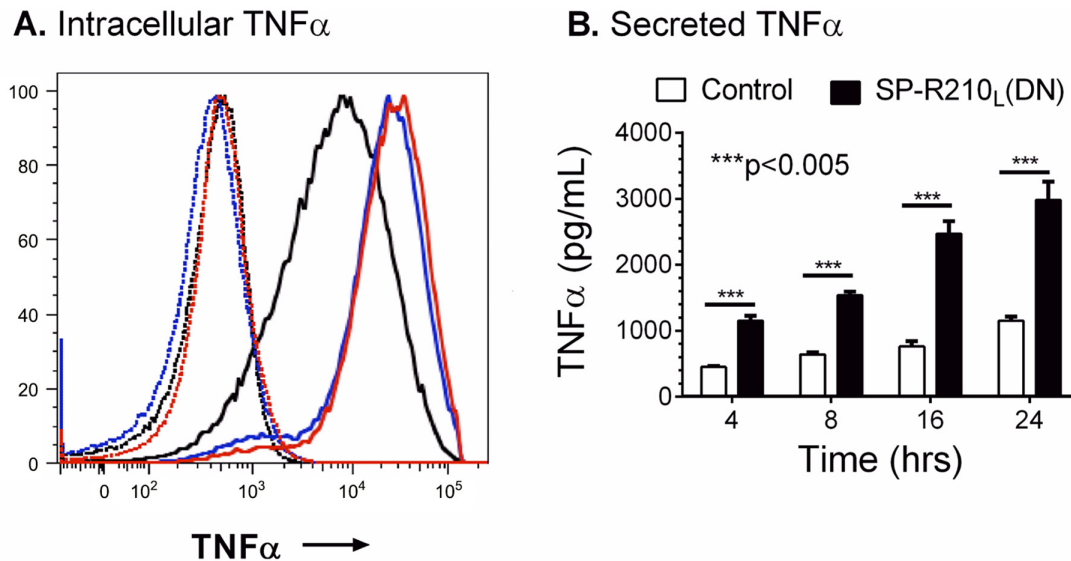


Fig 3. Increased responsiveness of SP-R210_L(DN) cells to LPS. Control and SPR210_L(DN) cells were plated in 12-well tissue culture dishes at a density of 150,000 cells/well and cultured 24 hrs in RPMI/10% FBS. Cells were then treated with 100 ng/mL LPS for 2, 4, 8, 16, and 24 hrs. A) Intracellular staining of TNF α was performed in brefeldin A blocked cells 2 hrs after treatment with LPS. Dotted histograms show untreated cells. Black, red, and blue histograms show intracellular TNF α staining of control, SP-R210_L(DN)1, and SP-R210_L(DN)2 cells. B) The levels of secreted TNF α were measured by ELISA in media at indicated time points after treatment with LPS. (n = 6; ***p<0.005).

doi:10.1371/journal.pone.0126576.g003

physical association between SP-R210_S and SR-A as well. In contrast, SP-R210 did not co-precipitate with CD36 and TLR-2 (Fig 5A) in neither control nor SP-R210_L(DN) cells, which serves as an internal control for specificity of SP-R210 interaction with CD14 and SR-A. Reciprocal immuno-precipitation assays using monoclonal CD11b antibodies (Fig 5B) shows that CD11b interacts preferentially with SP-R210_S in control cells. Interestingly, CD11b and SP-R210_S did not co-precipitate in SP-R210_L(DN) cells. As a member of the myosin family, SP-R210 is expected to form dimers via the carboxy-terminal coiled-coil domain. However, the preferential, albeit partial, interaction of CD11b with the short SP-R210_S but not the longer SP-R210_L isoform suggests that SP-R210_L and SP-R210_S do not form heterodimers with one another in macrophages [1]. Similar to SP-R210 (Fig 5A), CD11b did not associate with TLR-2 (Fig 5B) or with CD36 (not shown). Immunoprecipitation experiments using monoclonal antibodies to SP-R210 show that SP-R210_S and CD14 form a stable complex before and after treatment of cells with LPS over two hrs (Fig 5C). Interestingly, LPS treatment increased the level of immunoprecipitated SP-R210 isoforms over time. The level of co-precipitated CD14 in control cells was lower than in SP-R210_L(DN) cells, suggesting that SP-R210_L controls association of SP-R210_S with CD14 (Fig 5C).

To evaluate the functional significance of these interactions, we used antibodies to assess activation of macrophages by LPS (Fig 6). Cells were pre-treated with antibodies and then with 100 ng/mL LPS for 4 hrs followed by intracellular staining for TNF α . Pretreatment of macrophages with SP-R210 and CD11b antibodies did not affect TNF α synthesis in LPS-stimulated control cells. However, SR-A antibodies stimulated TNF α significantly in SP-R210_L(DN) compared to control cells by about 30% (Fig 6). CD14 antibodies blocked TNF α by 50% in both cell lines. Combined treatment with SP-R210 or SR-A antibodies interfered with the ability of CD14 antibodies to inhibit TNF α synthesis in SP-R210_L(DN) cells consistent with a close physical proximity between SP-R210_S, CD14 and SR-A in SP-R210_L(DN) cells as predicted by the immunoprecipitation results above. Consistent with a lack of interaction of SP-R210 with

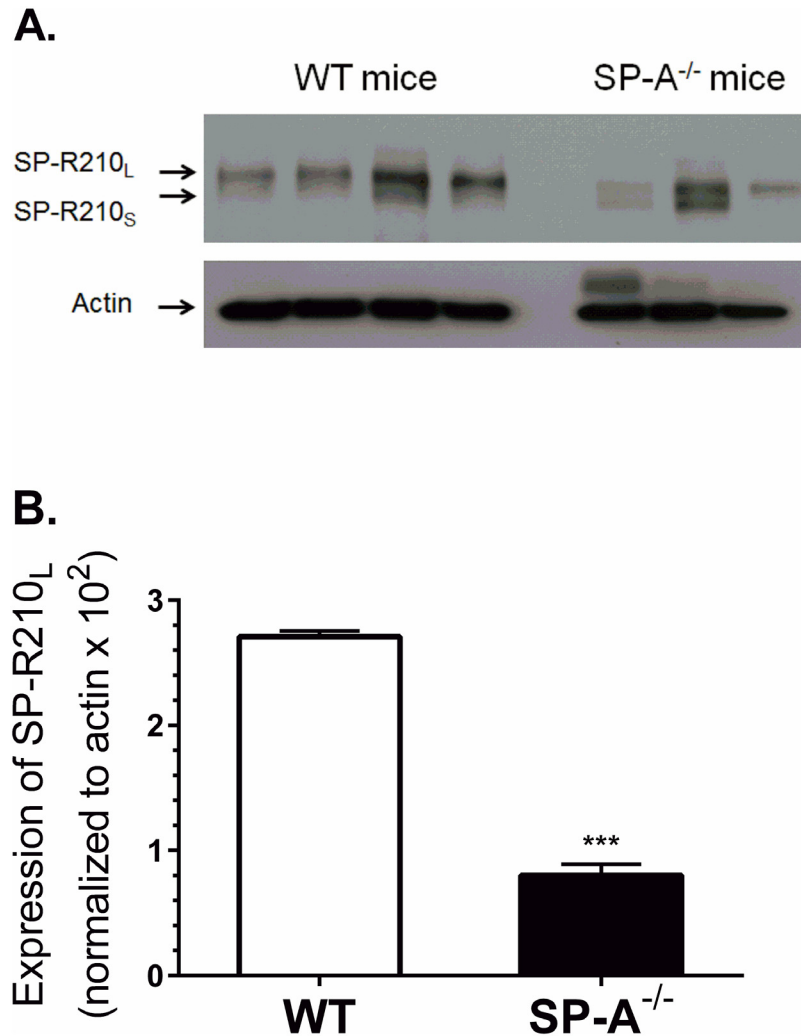


Fig 4. SP-A enhances expression of SP-R210_L in alveolar macrophages *in vivo*. Alveolar macrophages were isolated by lung lavage and processed for Western blot (A) and densitometry analysis (B) using polyclonal anti-SP-R210 antibodies. ****p*<0.001, *n* = 8 WT mice and *n* = 6 SP-A^{-/-} mice from two independent experiments.

doi:10.1371/journal.pone.0126576.g004

CD11b (Fig 5B), the CD11b antibody did not interfere with the CD14 inhibitory effect (Fig 6). Taken together these results indicate that SP-R210_L intrinsically regulates formation of pro-inflammatory innate immune receptor complexes between SP-R210_S, SR-A, and CD14.

SP-R210 isoforms regulate NFκB activation downstream of TLR-4

Previous studies have shown that LPS binds CD14 and transfers LPS to the toll-like receptor TLR-4 resulting in nuclear translocation and activation of the transcription factor NFκB [65]. The proximal TLR-4 signaling pathway involves myddosome formation followed by activation and degradation of IRAK-1 and downstream phosphorylation and degradation of IκB [66]. Degradation of IκB allows phosphorylation and translocation of NFκB p65 (RelA) subunit to the nucleus. Restoration of IκB expression contributes to termination of NFκB signaling [67]. Therefore, we determined whether lack of SP-R210_L alters TLR-4 signaling. The Western analysis on Fig 7A demonstrates that the kinetics of IRAK1 and IκB degradation were similar between

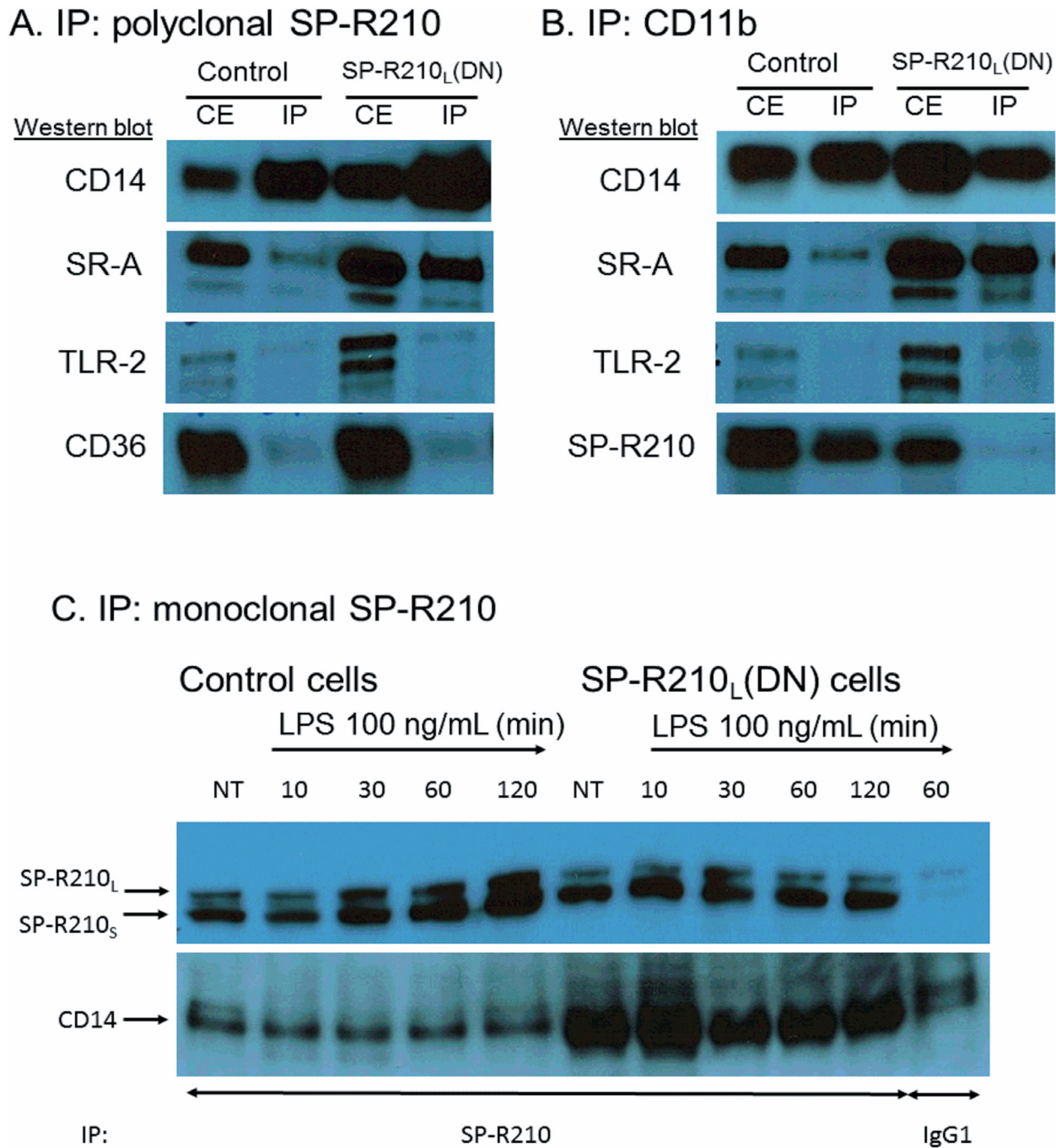


Fig 5. Interaction of SP-R210 with innate immune receptors. Immunoprecipitation experiments were carried out using 5 mg/mL (A and B) or 2.5 mg/mL (C) cell extracts from control and SP-R210_L(DN) macrophages with polyclonal anti-SP-R210 (A) or monoclonal CD11b (B). To assess the effect of LPS treatment, immunoprecipitation reactions were carried out 10, 30, 60, and 120 min after treatment with 100 ng/mL LPS (C). Co-precipitated proteins were separated on SDS-PAGE gels and blotted with indicated antibodies. Extracts immunoprecipitated with monoclonal anti-SP-R210 were re-probed with polyclonal SP-R210 antibodies. A monoclonal IgG1 against an unrelated viral antigen served as control (C). Results shown are representative of 2–4 independent experiments.

doi:10.1371/journal.pone.0126576.g005

control and SP-R210_L(DN) cells. Expression of IκB was restored after 30 min of LPS stimulation in both cell lines. However, the Western and densitometry analyses of Fig 7B and 7C demonstrated that phosphorylation of NFκB at serine 536 was transient in control cells but remained

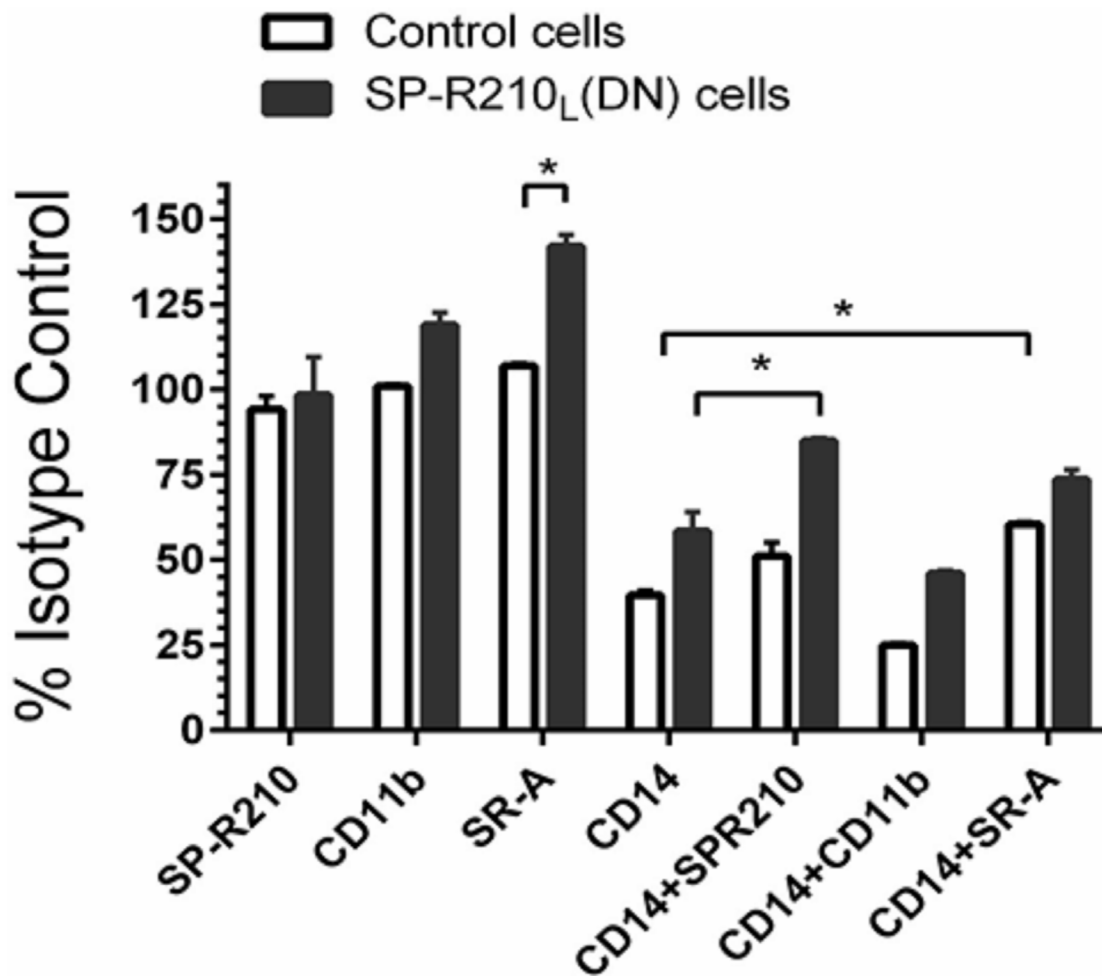


Fig 6. Effect of neutralizing antibodies on the inflammatory response to LPS. Control and SP-R210_L(DN) macrophages were pretreated for 60 min with 20 µg/mL of indicated individual or antibody combinations or respective isotype controls followed by stimulation with 100 ng/mL of LPS for 4 hrs. Cells were then harvested and processed for intracellular cytokine staining with TNFα antibodies. Stained cells were analyzed by flow cytometry. The mean fluorescence of positively stained cells was expressed as percent of isotype control treated cells. Data shown are means±SD and are pooled from 2–4 independent experiments performed in triplicate. *p<0.05.

doi:10.1371/journal.pone.0126576.g006

elevated in SP-R210_L(DN) cells. Furthermore, confocal fluorescent microscopy analysis on Fig 8A and 8B shows prolonged retention of NFκB in the nucleus of SP-R210_L(DN) cells compared to controls. These results indicate that SP-R210 regulates duration of NFκB signaling without affecting early signaling events of TLR-4 activation.

SP-R210_L and SP-R210_S mediate distinct internalization mechanisms of CD14

It has been demonstrated that CD14 controls internalization of TLR-4 which may determine TLR-4 activation from either the cell surface or endocytic vesicles [66]. CD14 was also shown to mediate macropinocytosis-mediated clearance of LPS [68]. We thus asked whether SP-R210 variants influence trafficking of CD14. Control and SP-R210_L(DN) macrophages were treated with 100 ng/mL LPS overtime to monitor internalization of CD14. Fig 9A demonstrates that 25% of CD14 was lost from the cell-surface by 2 hrs after addition of LPS and then new or recycled CD14 returned to the cell-surface by 4 hrs. In contrast, CD14 was replenished faster in

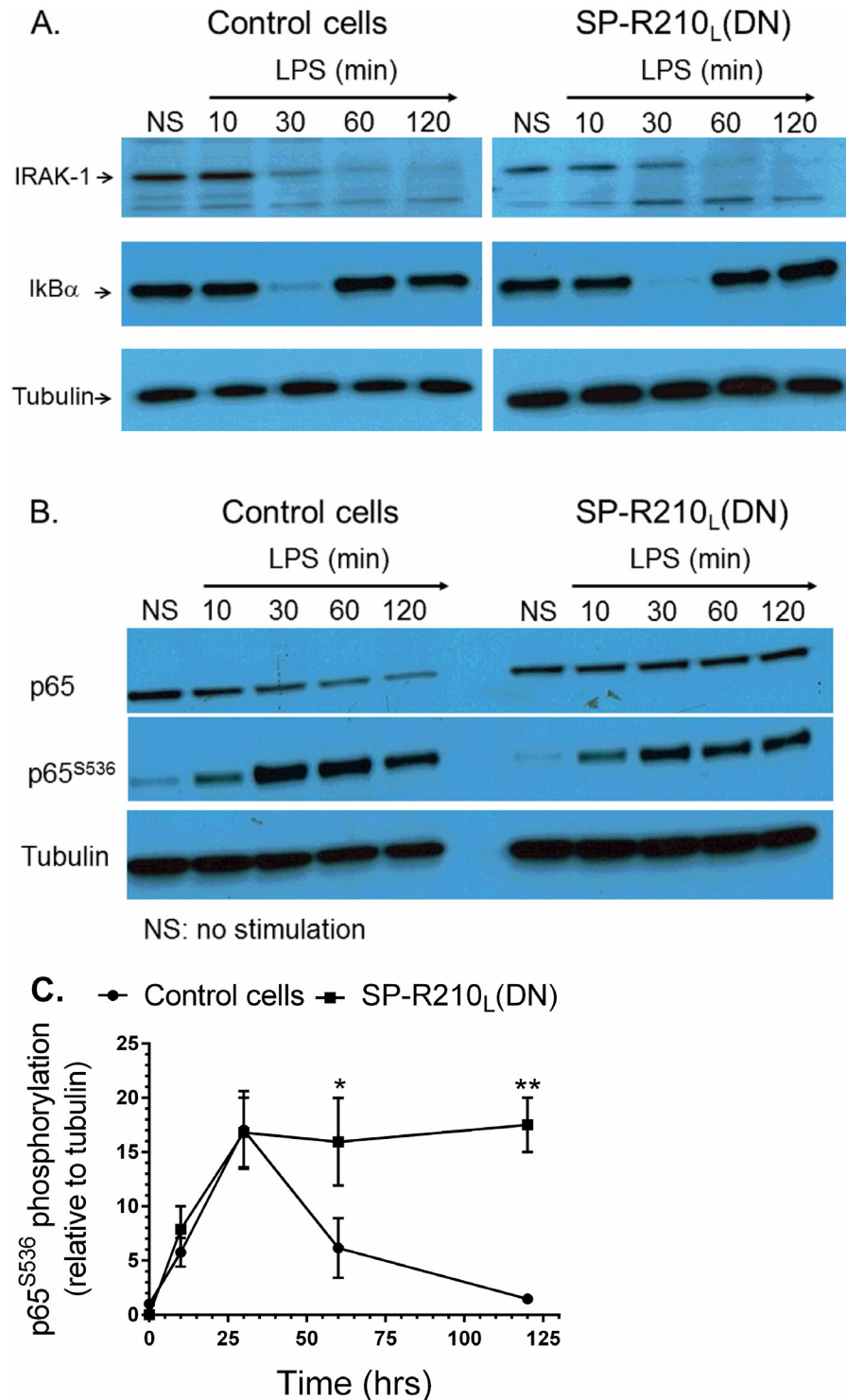
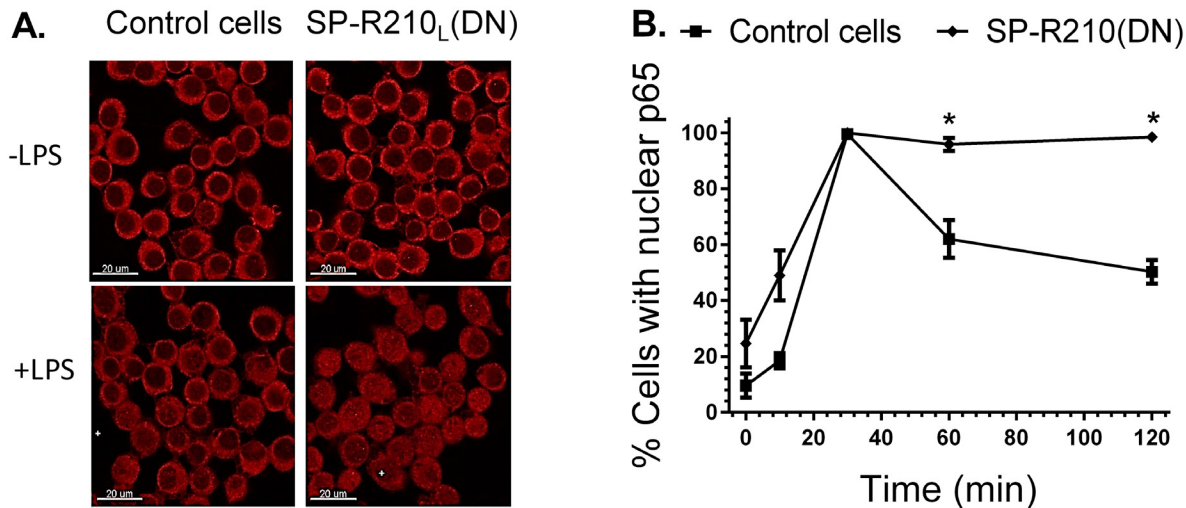


Fig 7. Activation of TLR4 signaling in control and SP-R210_L(DN) cells. Macrophages were stimulated with 100 ng/mL LPS and harvested at indicated time points. Non-stimulated (NS) and stimulated cells were harvested and processed for Western blot analysis. Blots were probed with IRAK-1 (A) or NFκB p65 (B) antibodies, stripped, and then re-probed with IκB or phosphorylated p65 antibodies, respectively. Blots were stripped and then re-probed with tubulin as loading control. Densitometry analysis compared the levels of phosphorylated p65 relative to tubulin (C). Blots in A and B are representative of 2–4 independent experiments. Data shown in C are means ± SD, n = 2- independent experiments. *p < 0.05.

doi:10.1371/journal.pone.0126576.g007



T = 120 min

Fig 8. Nuclear translocation of NFκB in control and SP-R210_L(DN) cells. Macrophages were grown on glass coverslips for 24 hrs, and then stimulated with 100 ng/mL LPS. Stimulated cells were then processed for immunofluorescent staining with anti-p65 NFκB at indicated time points after LPS treatment. The nuclear localization of NFκB was visualized by confocal microscopy (A). The percentage of cells containing nuclear p65 was quantitated in 10 random microscopic fields at 100 x magnification (B). Data shown are means±SD, n = 2 independent experiments performed in duplicate. *p<0.05.

doi:10.1371/journal.pone.0126576.g008

SP-R210_L(DN) cells (Fig 9A); only 15% of CD14 was lost from the cell-surface by 30 min with surface CD14 quickly returned to the cell-surface above the levels of unstimulated SP-R210_L(DN) cells. To probe the trafficking of CD14 further, we monitored surface CD14 after addition of dynasore, an inhibitor of clathrin and dynamin-dependent endocytosis [69]. Dynasore can also inhibit fluid phase endocytosis [70], endosomal recycling [71], and constitutive protein secretion in macrophages [70–72]. Fig 9B demonstrates that dynasore did not block internalization of CD14 in control cells, consistent with dynasore-insensitive macropinocytosis of CD14. However, dynasore blocked replenishment of surface CD14 completely in control cells and partially in SP-R210_L(DN) cells, suggesting that dynasore inhibits secretion of newly synthesized CD14. Dynasore, however, reveals a distinct trafficking process in SP-R210_L(DN) cells that is characterized by internalization over the first hour after addition of LPS followed by return of CD14 to the cell surface (Fig 9B), although additional studies will be needed to distinguish whether this represents dynasore-insensitive recycling or secretion of CD14. Differences in trafficking of CD14, however, do not impair endocytosis of TLR-4, although internalization of TLR-4 in SP-R210_L(DN) cells slowed after 1 hr of LPS compared to controls (Fig 9C). Dynasore has been shown to block endocytosis of TLR-4 inhibiting signaling from endocytic compartments [73]. CD14, however, was shown to mediate endocytosis of LPS via macropinocytosis [68]. Therefore, we compared the effects of dynasore and the macropinocytosis inhibitor EIPA [74] on the inflammatory response to LPS using intracellular TNFα as a readout of the LPS response. Fig 9D shows that dynasore and EIPA inhibited TNFα by 40 and 60%, respectively, indicating that internalization of CD14 is required to mediate part of the inflammatory response in control cells. In contrast, SP-R210_L(DN) cells were insensitive to inhibition by both dynasore and EIPA (Fig 9D). Previous studies have shown that the small GTPase Rac1 mediates macropinocytosis in macrophages [75, 76]. Accordingly, NSC23766 an inhibitor of the small GTPases Rac1 and Rac2 blocked TNFα production in both control and SP-R210_L(DN) cells. Interestingly, NSC23766 was significantly more effective at inhibiting TNFα in SP-R210_L(DN) compared to control cells (Fig 9D). Taken together, these results

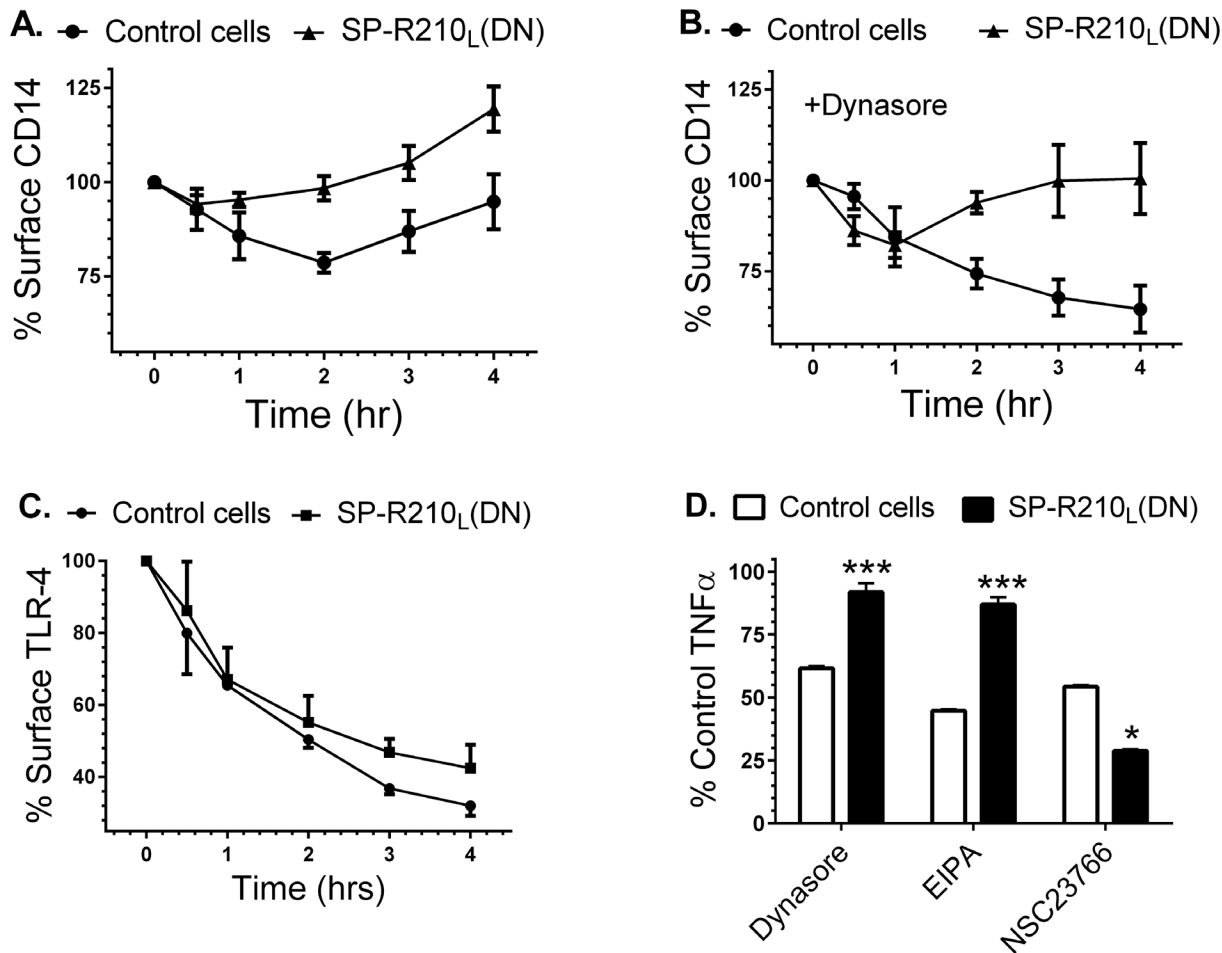


Fig 9. Effect of SP-R210_L disruption on CD14 and TLR-4 internalization and signaling. Macrophages cultured for 24 hrs on 12 well plates were simulated with 100 ng/mL LPS for indicated time points. The cells were then harvested at indicated time points using non-enzymatic cell displacement medium and stained with antibodies to CD14 (A and B) or TLR-4 (C). The effect of dynasore on internalization of CD14 (B) and of dynasore, EIPA, and NSC23766 on TNF α synthesis (D) was assessed by addition of inhibitors 30 min before addition of LPS. Harvested cells were analyzed by flow cytometry and mean fluorescence was expressed as % of control compared to non-stimulated control or SP-R210_L(DN) cells (t = 0) (A-C) or as percent of control TNF α in SP-R210_L(DN) cells compared to control cells (D). Data shown are means \pm SD, n = 2–4 independent experiments performed in triplicate. ***p<0.01, *p<0.04.

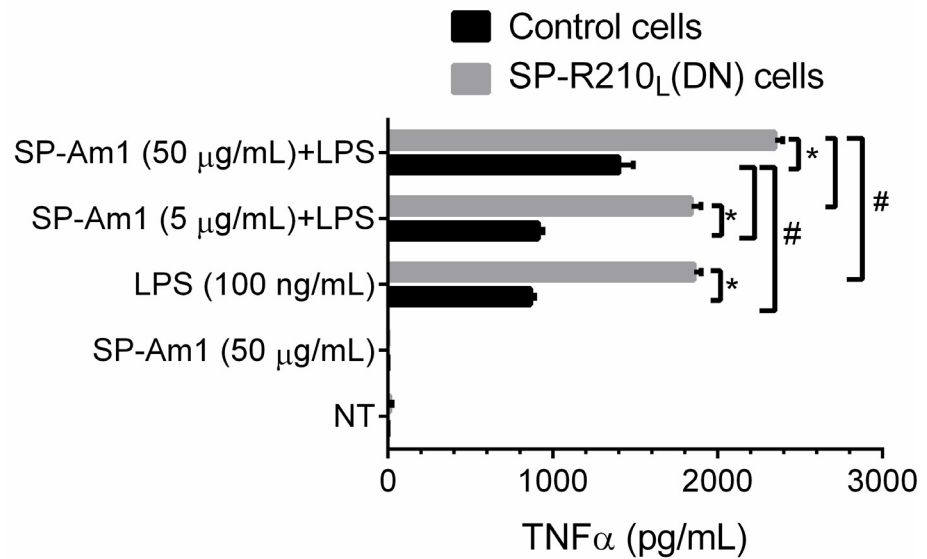
doi:10.1371/journal.pone.0126576.g009

indicate that SP-R210_L and SP-R210_S isoforms mediate trafficking of CD14 through distinct macropinocytosis-like mechanisms.

SP-A preparation influences responsiveness of macrophages to LPS

We then assessed whether SP-A modifies the inflammatory response to LPS. For these studies, we used SP-A from alveolar proteinosis fluid from the same individual purified by either a modified [57] butanol/octylglucoside method (SP-Am1) [58] or the isopropyl ether/butanol extraction method (SP-Am2) as recently described [48]; SP-Am1 as purified here has been shown to enhance macrophage activation [57, 77] whereas SP-Am2 was shown to be a potent antagonist of multiple toll-like receptors in several macrophage lines including Raw264.7 macrophages [48]. Control and SP-R210_L(DN) macrophages were exposed to low, 5 μ g/mL, or high, 50 μ g/mL, SP-Am1 for 24 hrs and subsequently incubated with 100 ng/mL of LPS (Fig 10A). Fig 10A shows that SP-Am1 enhanced responsiveness to LPS in both control and SP-R210_L(DN) cells.

A. SP-A-24 hrs → LPS-4 hrs



B. SP-A-24 hrs → LPS-4 hrs

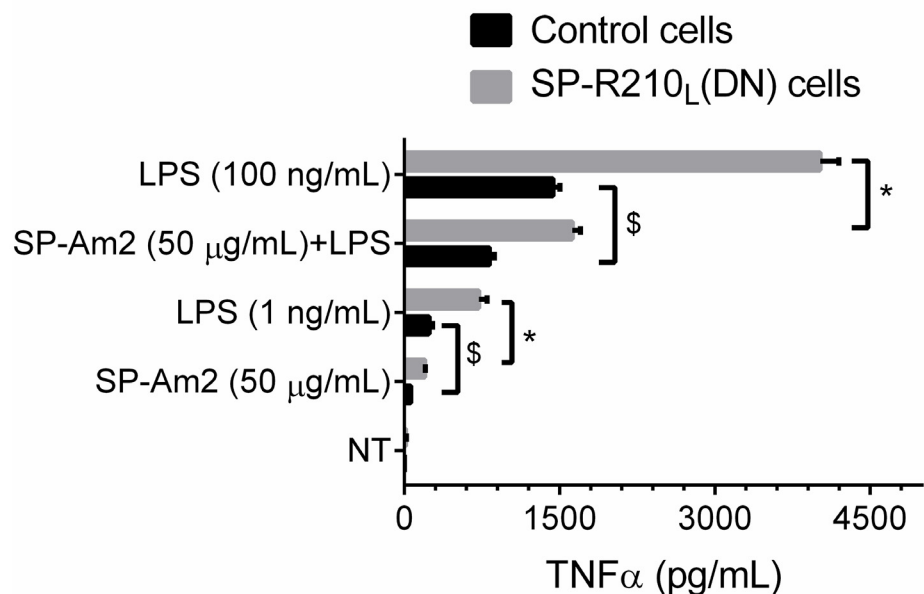


Fig 10. SP-A and SP-R210_L modulate responsiveness of macrophages to LPS. Control and SP-R210_L(DN) cells were pretreated with SP-A purified by either method 1 (SP-Am1) or method 2 (SP-Am2) as described in “Materials and Methods”. Cells were pretreated with indicated amounts of SP-Am1 (A) or SP-Am2 (B) for 24 hrs and then incubated with 100 ng/mL LPS. Levels of secreted TNFα were measured in media by ELISA at 4 hrs after addition of LPS. Data shown are means±SD, n = 3 representative of 3–6 independent experiments. Lines indicate significant differences between indicated groups at *p < 0.0001; #p < 0.04; \$p < 0.005

doi:10.1371/journal.pone.0126576.g010

SP-Am1 alone had no effect. However, SP-Am1 alone induced expression of CD14 in control cells but did not alter expression of CD14 in SP-R210_L(DN) cells (S2 Fig). The effect of SP-Am1 on LPS responsiveness appears long term since it was observed 24 hrs after LPS treatment (S3A

[Fig](#)). In contrast to SP-Am1, [Fig 10B](#) shows that SP-Am2 inhibited LPS-induced TNF α of both cell lines. The effect of SP-Am2 was examined at 50 μ g/mL concentration ([Fig 10B](#)). SP-Am2 contained measurable levels of LPS, which translates to 1 ng/mL LPS at the 50 μ g/mL SP-A dose. Compared to SP-Am1 alone that did not induce TNF α ([Fig 10A](#)), treatment with SP-Am2 produced measurable TNF α in both control and SP-R210_L(DN) although at 20–30% lower level of an equivalent amount of LPS alone ([Fig 10B](#)).

To address the different response to LPS in SP-Am1 and SP-Am2-treated macrophages, we evaluated the purity of SP-A preparations from the same and different individuals by silver staining, Western blot analysis, and mass spectrometry ([S4A–S4C Fig](#)). Silver-staining using the formaldehyde/glutaraldehyde based protocol of Rabiloud et al [59] revealed that SP-Am2 co-isolated with higher levels of low molecular weight proteins of approximately 8–15 kDa ([S4A Fig](#)) in the molecular range of surfactant protein B (SP-B). Of note, SP-B is not detectable by Coomassie blue staining [78] and thus SP-A preparations stained with Coomassie would appear pure. We obtained similar results with SP-A from three different individuals. Western blot analysis confirmed the presence of SP-B co-isolating with both SP-Am1 and SP-Am2, although clearly prominent in the SP-Am2 preparation ([S4B Fig](#)). Silver staining with the mass spectrometry compatible SilverQuest from Invitrogen revealed additional protein species above 300 kDa and proteins in the 8–25 kDa range ([S4C Fig](#)). The low molecular weight proteins are prominent in the SP-Am2 preparation with one protein in bands 5 and 6 that is present in one SP-Am1 and both SP-Am2 preparations ([S4C Fig](#)), respectively. These protein bands in SP-Am1 and SP-Am2 from APF-1 proteinosis material were in-gel digested and identified by MALDI mass spectrometry. The high molecular weight protein in bands 1 and 2 were similar in the two preparations and were both identified as gp340, a known binding protein for SP-A [79]. Band 3 contains a fragment of SP-A and ferritin light chain ([S4C Fig](#)), a previously described contaminant in SP-A preparations [5]. Ferritin light chain has been shown to suppress LPS-induced activation of macrophage [80]. Ferritin may contribute to the early inhibitory effect after brief 1 hr pre-treatment of macrophages with SP-Am1 and 4 hr stimulation with LPS ([S3B Fig](#)), although SP-Am1 retained its priming effect compared to SP-Am2 as observed 24 hrs after treatment with LPS ([S3B Fig](#)). Bands 4 in SP-Am1 and bands 6, 7, and 8 in SP-Am2 all contain SP-B. Band 5 contains the lung-specific aspartyl protease napsin A. In addition to SP-B, bands 6 and 7 also contain napsin A and the nuclear Histone H4, respectively. A blank piece of gel (band 10) did not yield any protein identifications. Intracellular napsin A has been shown to process pro-SPB in lamellar bodies of alveolar type II epithelial cells [81], although secreted napsin A may degrade cell surface proteins on alveolar cells [82]. The 30 kDa band 9 only contained SP-A as expected. All proteins were identified at 100% confidence index. These studies indicate that SP-A treatment leading to either enhanced or reduced responsiveness *in vitro* can depend in part on the level of co-isolating bioactive surfactant components or other molecules in different SP-A preparations.

Discussion

Precise regulation of the innate immune system is of paramount importance to respiratory health. Expression and sub-cellular localization of innate immune receptors determines the outcome of signaling responses that coordinate inflammation with clearance of pathogens. The present findings demonstrate that the SP-A receptor SP-R210_L isoform is an intrinsic modulator of innate immune receptors in macrophages. Multiple macrophage receptors have been shown to interact with SP-A [11, 25, 83], although the mechanisms by which SP-A modulates macrophage functions remain obscure. We found that SP-R210_L disruption leads to 2–20-fold increased expression of several innate immune receptors at both protein (TLR-2, CD11c, CD36,

and CD14) and transcriptional (SR-A, CD11b) levels. Studies on signaling pathways indicate that SP-R210_S and SP-R210_L control activation and deactivation of the transcription factor NFκB, respectively. Importantly, studies in alveolar macrophages from SP-A^{-/-} mice indicate that SP-A works in a paracrine fashion to maintain optimal expression levels of SP-R210_L [8], thereby modulating the functional phenotype of alveolar macrophages *in vivo*.

Our results indicate that SP-R210 isoforms regulate macrophage activation by CD14. Previous studies demonstrated that LPS binding to CD14 induces macropinocytosis and degradation of LPS in macrophages [68, 84, 85]. In turn, CD14 is required for LPS-induced endocytosis and activation of TLR-4 signaling in endosomes [66, 73]. Here, disruption of SP-R210_L revealed distinct mechanisms of CD14 uptake that modulate threshold and duration of macrophage activation in response to LPS. In addition to TLR-4 [65, 66, 86, 87], CD14 has also been shown to interact with TLR-2 [86, 88], CD36 [89], SR-A [89–91], and CD11b [92, 93], CD14 has been shown to coordinate ligand recognition, signaling and endocytosis of both TLR-4 [66, 73, 94–96] and TLR-2 [97, 98] via lipid raft-mediated and clathrin/dynamin-dependent endocytic mechanisms [99]. Other studies showed that CD36 partially facilitates macropinocytosis of LPS by CD14 while SR-A enhances expression of CD14 and TLR-4 [89]. Here, we found that SP-R210_S, CD14, and SR-A form a pro-inflammatory complex in SP-R210_L(DN) cells as revealed by functional assays using individual or a combination of neutralizing antibodies and immuno-precipitation experiments. Furthermore, we show different trafficking mechanisms of CD14 in control and SP-R210_L(DN) cells in which relocation or secretion of CD14 to the cell membrane after addition of LPS is dynasore-sensitive in control cells but dynasore-insensitive in SP-R210_L(DN) cells. Initial internalization of CD14 stimulated by LPS is insensitive to dynasore consistent with dynamin-independent internalization. Dynasore, however, partially inhibited LPS-induced TNFα in control cells only, consistent with inhibition of TLR-4 dynamin-dependent endocytosis and full activation of the inflammatory response by endosomal TLR-4 as expected based on previous reports [73]. Induction of TNFα by LPS was also inhibited by the hallmark macropinocytosis inhibitor EIPA in control cells, indicating that macropinocytic internalization of CD14 and/or TLR-4 is needed for downstream activation of the inflammatory response. EIPA and dynasore, however, had no effect on the LPS response in SP-R210_L(DN) cells, suggesting deployment of a novel inflammatory mechanism when SP-R210_L expression is attenuated. Interestingly, inhibition of the small GTPase Rac1 reduced LPS activation in both cells although more effectively in SP-R210_L(DN) cells, supporting the notion that Rac1 is a common downstream effector of LPS internalization and signaling. Rac1 is one of several GTPases that mediate macropinocytosis [75, 76, 100, 101]. On the other hand, Rac1 may contribute to prolonged activation of NFκB in SP-R210_L(DN) cells downstream of TLR-4 [102] or SR-A [103]. Taken together, the present findings support the notion that SP-R210_L plays a dominant intrinsic role to suppress inflammatory responsiveness of macrophages via a mechanism that modulates CD14 trafficking and cross-talk with the pro-inflammatory isoform SP-R210_S.

In the lung, SP-R210_L is the main isoform in alveolar macrophages. Earlier studies showed that SP-R210_L is induced in highly differentiated macrophages whereas SP-R210_S is expressed throughout the myeloid lineage [3]. Here, we show that SP-A enhances alveolar macrophage expression of SP-R210_L in the local environment. Recent studies showed that alveolar macrophages maintain a pro-inflammatory signature [104–106], indicating that alveolar macrophages are already primed for increased responsiveness to inflammatory agents *in vivo*. Conversely, alveolar macrophages are resistant to tolerogenic effects of LPS and other inflammatory stimuli [105, 107, 108]. Based on the present findings, we propose that SP-R210_L controls homeostatic functions of alveolar macrophages while low levels of SP-R210_S may be needed to initiate inflammatory responses rapidly.

In the present study we also sought to determine how SP-A affects macrophage responses to LPS in control and SP-R210_L(DN) cells. We found that treatment of macrophages with SP-A from the same individual prepared side-by-side by either modified butanol/octylglucoside [109] (SP-Am1) or isopropyl ether/butanol/ethanol extraction-based methods [48] (SP-Am2) results in priming [57] or suppression macrophage activation [48] by LPS, confirming earlier results with SP-A obtained by respective methods of purification from different individuals. The differential activities of SP-Am1 and SP-Am2 *in vitro* could be attributed to variable levels of co-isolating proteins that are known to contribute to surfactant function *in vivo* including gp340, a known surfactant protein binding protein [79], the pro-SP-B processing enzyme napsin A [81], and SP-B, which is crucial for surfactant function *in vivo* [53]. In the latter case, multiple studies in side-by-side or separate investigations have shown that Survanta, a clinically used surfactant preparation that contains SP-B and SP-C but not SP-A, exhibits anti-inflammatory activity in studies using mouse and human alveolar macrophages, peripheral blood monocytes, and monocytic cell lines [34, 46, 110–117]. In this regard, increasing studies indicate that SP-B and SP-C and surfactant lipids are not immunologically inert but rather act as antagonists of inflammation [11, 116, 118–120]. However, in an earlier study treatment of mice with SP-A purified by preparative isoelectric focusing had potent inflammatory properties using human monocytic cell lines *in vitro* [41–43, 46] over a number of years, but SP-A prepared in the same manner had anti-inflammatory activity when administered *in vivo* suppressing lung injury in the context of an adaptive immune response to allogeneic bone marrow transplant [121]. Interestingly, in the same injury model, side-by-side comparison with SP-A prepared by a commonly used isobutanol/octylglucoside that had anti-inflammatory properties *in vitro* also had anti-inflammatory activity *in vivo* [121]. In this regard, ligation of SP-R210 with an antibody that recognizes both isoforms resulted in secretion of IL-10 and TGFβ and suppression of lymphocyte proliferation in the context of a secondary immune response to mycobacterial antigen [12]. Taken together, variation in SP-A purity, co-isolating surfactant components, and the biological context in which SP-A is studied are important considerations in understanding SP-A functions *in vivo* and *in vitro*. It is reasonable to consider that co-isolating surfactant proteins contribute to anti-inflammatory activity of SP-A preparations by reducing binding of inflammatory agents to innate immune receptors, although these results may reflect physiological interactions of SP-A and SP-B *in vivo*. These findings highlight that extensive biochemical characterization of SP-A preparations is required to elucidate the interaction of SP-A with macrophage receptors.

Taken together, the present findings support the model depicted on Fig 11. In this model, SP-R210_L interacts with the Rac1 signaling pathway to enhance macropinocytosis and clearance of LPS via CD14 with moderate activation of endosomal TLR-4. We propose that the ability of SP-A to maintain high levels of SP-R210_L *in vivo* enhances the capacity of alveolar macrophages to clear LPS without overt inflammation, providing a mechanistic explanation for the anti-inflammatory role of SP-A *in vivo*. In turn, SP-R210_L modulates expression and localization of innate immune receptors priming macrophages for an appropriate response at increased levels of inflammatory agents in the environment. However, in the absence of SP-R210_L-mediated regulation, the response to LPS is mediated through a pro-inflammatory complex between SP-R210_S, CD14, and SR-A in which SR-A is responsible for macropinocytosis-like internalization of LPS and prolonged activation of the rac-1 signaling pathway. In this case, SP-A and possibly other surfactant components may serve to inhibit the SP-R210_S/CD14/SR-A complex, contributing to regulation and resolution of the inflammatory response. This model is supported by endocytic, biochemical, and functional assays utilizing neutralizing antibodies to SP-R210 and co-receptors and small molecule inhibitors. Domain and isoform specific monoclonal antibodies will help define the expression and function of SP-R210 isoforms in different macrophage populations in the

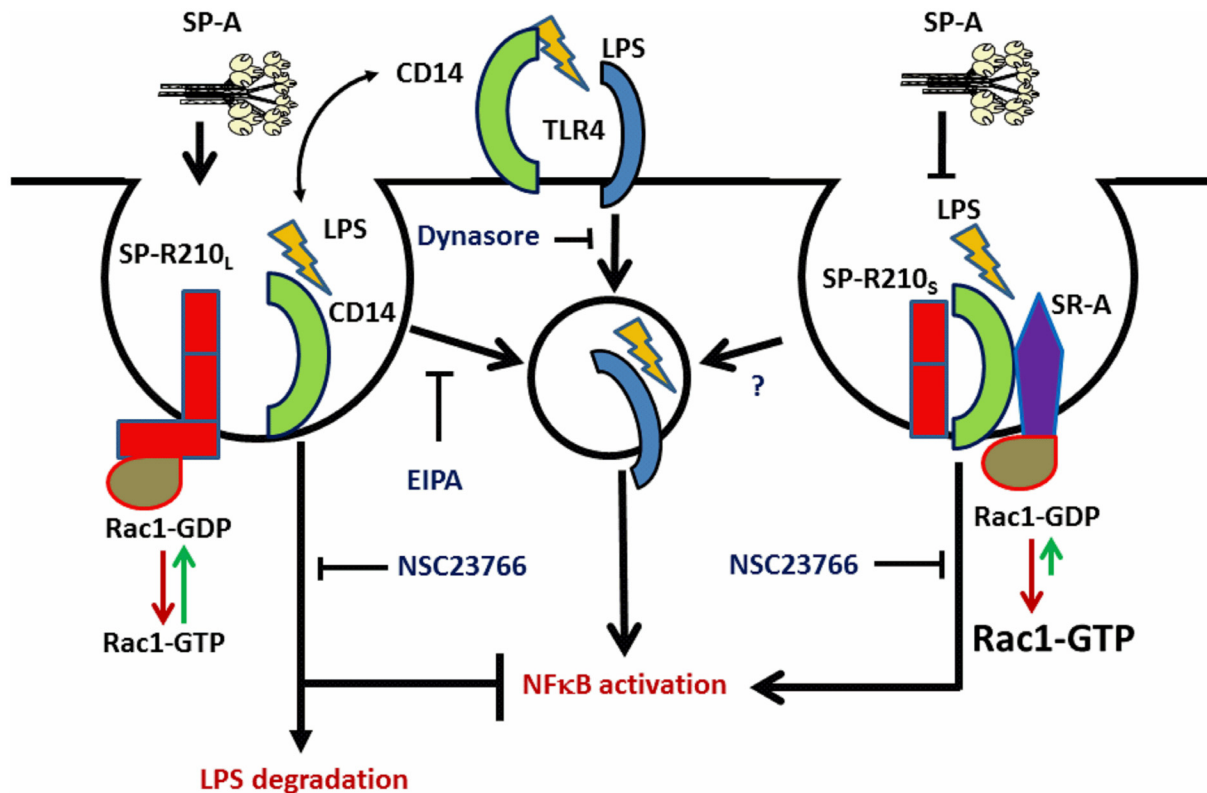


Fig 11. Proposed interaction of SP-R210 isoforms with CD14 and SR-A in macrophage activation. SP-R210_L mediates macropinocytosis of LPS-CD14 through interaction with Rac1 resulting in endosomal LPS delivery to TLR-4 and downstream activation of NFκB. Subsequent degradation of LPS results in decrease NFκB signaling. SP-R210_L-mediated macropinocytosis and signaling are sensitive to both EIPA and NSC23766. TLR-4 signaling from the cell-surface is sensitive to dynasore. Inhibition of SP-R210_L expression results in formation of the SP-R210_S-CD14-SR-A complex. Binding of LPS results in macropinocytosis-like internalization of the SP-R210_S-CD14-SR-A complex and activation of a feed-forward inflammatory pathway that depends on activation of Rac1 by SR-A. The SP-R210_S-CD14-SR-A pathway is sensitive to NSC23766 but not EIPA.

doi:10.1371/journal.pone.0126576.g011

future. SP-R210_L is the main isoform on alveolar macrophages [5], indicating that expression of SP-R210_L is regulated locally. Our study suggests that differential expression of SP-R210 isoforms determines the inflammatory phenotype of macrophages.

Supporting Information

S1 Fig. SP-A induces expression of SP-R210. Expression of SP-R210 was determined by Western blot analysis in control (A) and SP-R210_L(DN) (B) cells treated with increasing concentration of SP-A purified by method 1. The cells were also treated with 100 ng/mL LPS. Blots were re-probed with actin as loading control. Control (A) and SP-R210_L(DN) (B) cells were cultured in 12 well plates for 24 hrs and then treated with increasing concentrations of SP-A, or 100 ng/mL LPS. The band intensity of SP-R210_L, SP-R210_S, and actin was determined by densitometry. Densitometry data were normalized to actin and expressed relative to SP-R210_L in untreated (NT) control cells (A) and SP-R210_S in SP-R210_L(DN) (B) cells. Data shown are representative of two independent experiments SP-Am1. (TIF)

S2 Fig. SP-A and LPS enhance expression of CD14. Expression of CD14 was determined by Western blot analysis in control (B) and SP-R210_L(DN) (B) cells treated with increasing concentration of SP-A purified by method 1 or 100 ng/mL LPS for 24 hrs. Blots were re-probed

with actin as loading control. The band intensity of CD14 and actin was determined by densitometry. Densitometry data were normalized to actin and expressed relative to CD14 in untreated (NT) cells. Data shown are representative of two independent experiments using SP-Am1.

(TIF)

S3 Fig. SP-A preparations enhance or inhibit responsiveness of macrophages to LPS. Control and SP-R210_i(DN) cells were pretreated with SP-A purified by either method 1 (SP-Am1) or method 2 (SP-Am2) as described in “Materials and methods”. A) Cells were pretreated with 5 or 50 µg/mL SP-Am1 for 24 hrs and then incubated with 100 ng/mL LPS. Levels of secreted TNFα were measured in media by ELISA at 24 (B) hrs after addition of LPS. B) To measure the effect of SP-A purified by different methods, control cells were pre-incubated for 1 hr with 50 µg/mL SP-Am1 or SP-Am2 and then treated with 100 ng/mL LPS. Secretion of TNFα was measured 4 and 24 hrs after addition of LPS. *p < 0.0001; #p < 0.04; \$p < 0.005

(TIF)

S4 Fig. Isolation and characterization of SP-A by different methods. SP-A was purified from alveolar proteinosis fluid (APF) obtained by therapeutic lung lavage from different alveolar proteinosis patients using methods 1 and 2 as described in “Materials and Methods”. (A) The purity of SP-A was assessed by silver staining as described by Rabiloud [59]. (B) The presence of SP-B was verified by Western blot analysis. Proteins were separated on reducing (A) or non-reducing (B) 4–17% SDS-PAGE gels. SP-A purified by both methods were free of SP-D (not shown). Arrows indicate positions of SP-B and SP-A. (C) SP-A preparations separated on reducing SDS-PAGE were stained using the Invitrogen SilverQuest kit suitable for mass spectrometry. Gel bands were identified by numbers were subjected to in-trypsin digests and tryptic peptide fingerprints and interrogated by MALDI mass spectrometry. Proteins found in each gel band were identified at 100% confidence index.

(TIF)

Author Contributions

Conceived and designed the experiments: ZCC LY MC NDC. Performed the experiments: YMW SLD PS TMU ESH LY SH MLD ZCC. Analyzed the data: ZCC YMW PS TMU LY. Contributed reagents/materials/analysis tools: ZCC JF PS NDC FXM. Wrote the paper: ZCC. Critical manuscript reading: ZCC JF ESH TMU PS YMW NDC MLD MC LY.

References

1. Mori K, Matsuda K, Furusawa T, Kawata M, Inoue T, Obinata M. Subcellular localization and dynamics of MysPDZ (Myo18A) in live mammalian cells. *Biochem Biophys Res Commun*. 2005; 326(2):491–8. Epub 2004/12/08. doi: [10.1016/j.bbrc.2004.11.058](https://doi.org/10.1016/j.bbrc.2004.11.058) PMID: [15582604](https://pubmed.ncbi.nlm.nih.gov/15582604/).
2. Cross M, Csar XF, Wilson NJ, Manes G, Addona TA, Marks DC, et al. A novel 110 kDa form of myosin XVIII A (MysPDZ) is tyrosine-phosphorylated after colony-stimulating factor-1 receptor signalling. *Biochem J*. 2004; 380(Pt 1):243–53. Epub 2004/02/19. doi: [10.1042/BJ20031978](https://doi.org/10.1042/BJ20031978) PMID: [14969583](https://pubmed.ncbi.nlm.nih.gov/14969583/); PubMed Central PMCID: [PMC1224155](https://pubmed.ncbi.nlm.nih.gov/PMC1224155/).
3. Mori K, Furusawa T, Okubo T, Inoue T, Ikawa S, Yanai N, et al. Genome structure and differential expression of two isoforms of a novel PDZ-containing myosin (MysPDZ) (Myo18A). *Journal of biochemistry*. 2003; 133(4):405–13. Epub 2003/05/23. PMID: [12761286](https://pubmed.ncbi.nlm.nih.gov/12761286/).
4. Furusawa T, Ikawa S, Yanai N, Obinata M. Isolation of a novel PDZ-containing myosin from hematopoietic supportive bone marrow stromal cell lines. *Biochem Biophys Res Commun*. 2000; 270(1):67–75. Epub 2000/03/29. doi: [10.1006/bbrc.2000.2377](https://doi.org/10.1006/bbrc.2000.2377) PMID: [10733906](https://pubmed.ncbi.nlm.nih.gov/10733906/).
5. Yang CH, Szeliga J, Jordan J, Faske S, Sever-Chroneos Z, Dorsett B, et al. Identification of the surfactant protein A receptor 210 as the unconventional myosin 18A. *J Biol Chem*. 2005; 280(41):34447–

57. Epub 2005/08/10. doi: [10.1074/jbc.M505229200](https://doi.org/10.1074/jbc.M505229200) PMID: [16087679](https://pubmed.ncbi.nlm.nih.gov/16087679/); PubMed Central PMCID: PMC1762002.
6. Szeliga J, Jordan J, Yang CH, Sever-Chroneos Z, Chroneos ZC. Bacterial expression of recombinant MyoXVIIIa domains. *Anal Biochem.* 2005; 346(1):179–81. Epub 2005/09/27. doi: [10.1016/j.ab.2005.07.021](https://doi.org/10.1016/j.ab.2005.07.021) PMID: [16183031](https://pubmed.ncbi.nlm.nih.gov/16183031/); PubMed Central PMCID: PMC1633724.
7. Guzik-Lendrum S, Nagy A, Takagi Y, Houdusse A, Sellers JR. *Drosophila melanogaster* myosin-18 represents a highly divergent motor with actin tethering properties. *J Biol Chem.* 2011; 286(24):21755–66. Epub 2011/04/19. doi: [10.1074/jbc.M111.218669](https://doi.org/10.1074/jbc.M111.218669) PMID: [21498886](https://pubmed.ncbi.nlm.nih.gov/21498886/); PubMed Central PMCID: PMC3122231.
8. Sever-Chroneos Z, Krupa A, Davis J, Hasan M, Yang CH, Szeliga J, et al. Surfactant protein A (SP-A)-mediated clearance of *Staphylococcus aureus* involves binding of SP-A to the staphylococcal adhesin eap and the macrophage receptors SP-A receptor 210 and scavenger receptor class A. *J Biol Chem.* 2011; 286(6):4854–70. Epub 2010/12/03. doi: [10.1074/jbc.M110.125567](https://doi.org/10.1074/jbc.M110.125567) PMID: [21123169](https://pubmed.ncbi.nlm.nih.gov/21123169/); PubMed Central PMCID: PMC3039347.
9. Matsui K, Parameswaran N, Bagheri N, Willard B, Gupta N. Proteomics analysis of the ezrin interactome in B cells reveals a novel association with Myo18aalpha. *J Proteome Res.* 2011; 10(9):3983–92. Epub 2011/07/15. doi: [10.1021/pr200577d](https://doi.org/10.1021/pr200577d) PMID: [21751808](https://pubmed.ncbi.nlm.nih.gov/21751808/); PubMed Central PMCID: PMC3181492.
10. Isogawa Y, Kon T, Inoue T, Ohkura R, Yamakawa H, Ohara O, et al. The N-terminal domain of MYO18A has an ATP-insensitive actin-binding site. *Biochemistry.* 2005; 44(16):6190–6. Epub 2005/04/20. doi: [10.1021/bi0475931](https://doi.org/10.1021/bi0475931) PMID: [15835906](https://pubmed.ncbi.nlm.nih.gov/15835906/).
11. Chroneos ZC, Sever-Chroneos Z, Shepherd VL. Pulmonary surfactant: an immunological perspective. *Cell Physiol Biochem.* 2010; 25(1):13–26. doi: [10.1159/000272047](https://doi.org/10.1159/000272047) PMID: [20054141](https://pubmed.ncbi.nlm.nih.gov/20054141/); PubMed Central PMCID: PMC3025886.
12. Samten B, Townsend JC, Sever-Chroneos Z, Pasquinelli V, Barnes PF, Chroneos ZC. An antibody against the surfactant protein A (SP-A)-binding domain of the SP-A receptor inhibits T cell-mediated immune responses to *Mycobacterium tuberculosis*. *J Leukoc Biol.* 2008; 84(1):115–23. doi: [10.1189/jlb.1207835](https://doi.org/10.1189/jlb.1207835) PMID: [18443188](https://pubmed.ncbi.nlm.nih.gov/18443188/); PubMed Central PMCID: PMC3178510.
13. Weikert LF, Lopez JP, Abdolrasulnia R, Chroneos ZC, Shepherd VL. Surfactant protein A enhances mycobacterial killing by rat macrophages through a nitric oxide-dependent pathway. *Am J Physiol Lung Cell Mol Physiol.* 2000; 279(2):L216–23. Epub 2000/08/05. PMID: [10926544](https://pubmed.ncbi.nlm.nih.gov/10926544/).
14. Borron P, McCormack FX, Elhalwagi BM, Chroneos ZC, Lewis JF, Zhu S, et al. Surfactant protein A inhibits T cell proliferation via its collagen-like tail and a 210-kDa receptor. *Am J Physiol.* 1998; 275(4 Pt 1):L679–86. PMID: [9755099](https://pubmed.ncbi.nlm.nih.gov/9755099/).
15. Weikert LF, Edwards K, Chroneos ZC, Hager C, Hoffman L, Shepherd VL. SP-A enhances uptake of bacillus Calmette-Guerin by macrophages through a specific SP-A receptor. *Am J Physiol.* 1997; 272(5 Pt 1):L989–95. Epub 1997/05/01. PMID: [9176265](https://pubmed.ncbi.nlm.nih.gov/9176265/).
16. Chroneos ZC, Abdolrasulnia R, Whitsett JA, Rice WR, Shepherd VL. Purification of a cell-surface receptor for surfactant protein A. *J Biol Chem.* 1996; 271(27):16375–83. PMID: [8663107](https://pubmed.ncbi.nlm.nih.gov/8663107/).
17. Canadas O, Keough KM, Casals C. Bacterial lipopolysaccharide promotes destabilization of lung surfactant-like films. *Biophysical journal.* 2011; 100(1):108–16. Epub 2010/12/31. doi: [10.1016/j.bpj.2010.11.028](https://doi.org/10.1016/j.bpj.2010.11.028) PMID: [21190662](https://pubmed.ncbi.nlm.nih.gov/21190662/); PubMed Central PMCID: PMC3010832.
18. Nagy A, Takagi Y, Billington N, Sun SA, Hong DK, Homsher E, et al. Kinetic characterization of non-muscle Myosin IIb at the single molecule level. *J Biol Chem.* 2013; 288(1):709–22. Epub 2012/11/14. doi: [10.1074/jbc.M112.424671](https://doi.org/10.1074/jbc.M112.424671) PMID: [23148220](https://pubmed.ncbi.nlm.nih.gov/23148220/); PubMed Central PMCID: PMC3537070.
19. Byron A, Humphries JD, Craig SE, Knight D, Humphries MJ. Proteomic analysis of alpha4beta1 integrin adhesion complexes reveals alpha-subunit-dependent protein recruitment. *Proteomics.* 2012; 12(13):2107–14. Epub 2012/05/25. doi: [10.1002/pmic.201100487](https://doi.org/10.1002/pmic.201100487) PMID: [22623428](https://pubmed.ncbi.nlm.nih.gov/22623428/); PubMed Central PMCID: PMC3472074.
20. Bishe B, Syed GH, Field SJ, Siddiqui A. Role of phosphatidylinositol 4-phosphate (PI4P) and its binding protein GOLPH3 in hepatitis C virus secretion. *J Biol Chem.* 2012; 287(33):27637–47. Epub 2012/06/30. doi: [10.1074/jbc.M112.346569](https://doi.org/10.1074/jbc.M112.346569) PMID: [22745132](https://pubmed.ncbi.nlm.nih.gov/22745132/); PubMed Central PMCID: PMC3431621.
21. Dippold HC, Ng MM, Farber-Katz SE, Lee SK, Kerr ML, Peterman MC, et al. GOLPH3 bridges phosphatidylinositol-4-phosphate and actomyosin to stretch and shape the Golgi to promote budding. *Cell.* 2009; 139(2):337–51. Epub 2009/10/20. doi: [10.1016/j.cell.2009.07.052](https://doi.org/10.1016/j.cell.2009.07.052) PMID: [19837035](https://pubmed.ncbi.nlm.nih.gov/19837035/); PubMed Central PMCID: PMC2779841.
22. Tan I, Yong J, Dong JM, Lim L, Leung T. A tripartite complex containing MRCK modulates lamellar actomyosin retrograde flow. *Cell.* 2008; 135(1):123–36. Epub 2008/10/16. doi: [10.1016/j.cell.2008.09.018](https://doi.org/10.1016/j.cell.2008.09.018) PMID: [18854160](https://pubmed.ncbi.nlm.nih.gov/18854160/).
23. Hsu RM, Tsai MH, Hsieh YJ, Lyu PC, Yu JS. Identification of MYO18A as a novel interacting partner of the PAK2/betaPIX/GIT1 complex and its potential function in modulating epithelial cell migration.

- Mol Biol Cell. 2010; 21(2):287–301. doi: [10.1091/mbc.E09-03-0232](https://doi.org/10.1091/mbc.E09-03-0232) PMID: [19923322](https://pubmed.ncbi.nlm.nih.gov/19923322/); PubMed Central PMCID: PMC2808764.
24. Lopez-Sanchez A, Saenz A, Casals C. Surfactant protein A (SP-A)-tacrolimus complexes have a greater anti-inflammatory effect than either SP-A or tacrolimus alone on human macrophage-like U937 cells. *Eur J Pharm Biopharm.* 2010. Epub 2010/12/22. doi: [10.1016/j.ejpb.2010.12.013](https://doi.org/10.1016/j.ejpb.2010.12.013) PMID: [21172435](https://pubmed.ncbi.nlm.nih.gov/21172435/).
 25. Nayak A, Dodagatta-Marri E, Tsolaki AG, Kishore U. An Insight into the Diverse Roles of Surfactant Proteins, SP-A and SP-D in Innate and Adaptive Immunity. *Frontiers in immunology.* 2012; 3:131. Epub 2012/06/16. doi: [10.3389/fimmu.2012.00131](https://doi.org/10.3389/fimmu.2012.00131) PMID: [22701116](https://pubmed.ncbi.nlm.nih.gov/22701116/); PubMed Central PMCID: PMC3369187.
 26. Tenner AJ, Robinson SL, Borchelt J, Wright JR. Human pulmonary surfactant protein (SP-A), a protein structurally homologous to C1q, can enhance FcR- and CR1-mediated phagocytosis. *J Biol Chem.* 1989; 264(23):13923–8. Epub 1989/08/15. PMID: [2788165](https://pubmed.ncbi.nlm.nih.gov/2788165/).
 27. Gil M, McCormack FX, Levine AM. Surfactant protein-A modulates cell surface expression of CR3 on alveolar macrophages and enhances CR3-mediated phagocytosis. *J Biol Chem.* 2009. Epub 2009/01/22. doi: [10.1074/jbc.M808643200](https://doi.org/10.1074/jbc.M808643200) [pii]doi: [10.1074/jbc.M808643200](https://doi.org/10.1074/jbc.M808643200) PMID: [19155216](https://pubmed.ncbi.nlm.nih.gov/19155216/).
 28. Beharka AA, Crowther JE, McCormack FX, Denning GM, Lees J, Tibesar E, et al. Pulmonary surfactant protein A activates a phosphatidylinositol 3-kinase/calcium signal transduction pathway in human macrophages: participation in the up-regulation of mannose receptor activity. *J Immunol.* 2005; 175(4):2227–36. Epub 2005/08/06. doi: [175/4/2227](https://doi.org/10.1172/JCI2227) [pii]. PMID: [16081790](https://pubmed.ncbi.nlm.nih.gov/16081790/).
 29. Gaynor CD, McCormack FX, Voelker DR, McGowan SE, Schlesinger LS. Pulmonary surfactant protein A mediates enhanced phagocytosis of Mycobacterium tuberculosis by a direct interaction with human macrophages. *J Immunol.* 1995; 155(11):5343–51. PMID: [7594549](https://pubmed.ncbi.nlm.nih.gov/7594549/).
 30. Kuronuma K, Sano H, Kato K, Kudo K, Hyakushima N, Yokota S, et al. Pulmonary surfactant protein A augments the phagocytosis of Streptococcus pneumoniae by alveolar macrophages through a casein kinase 2-dependent increase of cell surface localization of scavenger receptor A. *J Biol Chem.* 2004; 279(20):21421–30. PMID: [14993215](https://pubmed.ncbi.nlm.nih.gov/14993215/).
 31. Ketko AK, Lin C, Moore BB, LeVine AM. Surfactant protein A binds flagellin enhancing phagocytosis and IL-1beta production. *PLoS One.* 2013; 8(12):e82680. doi: [10.1371/journal.pone.0082680](https://doi.org/10.1371/journal.pone.0082680) PMID: [24312669](https://pubmed.ncbi.nlm.nih.gov/24312669/); PubMed Central PMCID: PMC3846784.
 32. Gardai SJ, Xiao YQ, Dickinson M, Nick JA, Voelker DR, Greene KE, et al. By binding SIRPalpha or calreticulin/CD91, lung collectins act as dual function surveillance molecules to suppress or enhance inflammation. *Cell.* 2003; 115(1):13–23. PMID: [14531999](https://pubmed.ncbi.nlm.nih.gov/14531999/).
 33. Janssen WJ, McPhillips KA, Dickinson MG, Linderman DJ, Morimoto K, Xiao YQ, et al. Surfactant proteins A and D suppress alveolar macrophage phagocytosis via interaction with uki alpha. *Am J Respir Crit Care Med.* 2008; 178(2):158–67. Epub 2008/04/19. doi: [10.1164/rccm.200711-1661OC](https://doi.org/10.1164/rccm.200711-1661OC) PMID: [18420961](https://pubmed.ncbi.nlm.nih.gov/18420961/); PubMed Central PMCID: PMC2453510.
 34. Nguyen HA, Rajaram MV, Meyer DA, Schlesinger LS. Pulmonary surfactant protein A and surfactant lipids upregulate IRAK-M, a negative regulator of TLR-mediated inflammation in human macrophages. *Am J Physiol Lung Cell Mol Physiol.* 2012; 303(7):L608–16. Epub 2012/08/14. doi: [10.1152/ajplung.00067.2012](https://doi.org/10.1152/ajplung.00067.2012) PMID: [22886503](https://pubmed.ncbi.nlm.nih.gov/22886503/); PubMed Central PMCID: PMC3469587.
 35. Garcia-Verdugo I, Sanchez-Barbero F, Soldau K, Tobias PS, Casals C. Interaction of SP-A (surfactant protein A) with bacterial rough lipopolysaccharide (Re-LPS), and effects of SP-A on the binding of Re-LPS to CD14 and LPS-binding protein. *Biochem J.* 2005; 391(Pt 1):115–24. Epub 2005/06/04. doi: [10.1042/BJ20050529](https://doi.org/10.1042/BJ20050529) PMID: [15932345](https://pubmed.ncbi.nlm.nih.gov/15932345/); PubMed Central PMCID: PMC1237145.
 36. Sano H, Chiba H, Iwaki D, Sohma H, Voelker DR, Kuroki Y. Surfactant proteins A and D bind CD14 by different mechanisms. *J Biol Chem.* 2000; 275(29):22442–51. PMID: [10801802](https://pubmed.ncbi.nlm.nih.gov/10801802/).
 37. Sano H, Sohma H, Muta T, Nomura S, Voelker DR, Kuroki Y. Pulmonary surfactant protein A modulates the cellular response to smooth and rough lipopolysaccharides by interaction with CD14. *J Immunol.* 1999; 163(1):387–95. Epub 1999/06/29. doi: [ji_v163n1p387](https://doi.org/10.1172/JCI10384) [pii]. PMID: [10384140](https://pubmed.ncbi.nlm.nih.gov/10384140/).
 38. Ramani V, Madhusoodhanan R, Kosanke S, Awasthi S. A TLR4-interacting SPA4 peptide inhibits LPS-induced lung inflammation. *Innate Immun.* 2013; 19(6):596–610. doi: [10.1177/1753425912474851](https://doi.org/10.1177/1753425912474851) PMID: [23475791](https://pubmed.ncbi.nlm.nih.gov/23475791/).
 39. Yamada C, Sano H, Shimizu T, Mitsuzawa H, Nishitani C, Himi T, et al. Surfactant protein A directly interacts with TLR4 and MD-2 and regulates inflammatory cellular response. Importance of supratrimeric oligomerization. *J Biol Chem.* 2006; 281(31):21771–80. Epub 2006/06/07. doi: [10.1074/jbc.M513041200](https://doi.org/10.1074/jbc.M513041200) PMID: [16754682](https://pubmed.ncbi.nlm.nih.gov/16754682/).
 40. Sender V, Lang L, Stamme C. Surfactant Protein-A Modulates LPS-Induced TLR4 Localization and Signaling via beta-Arrestin 2. *PLoS One.* 2013; 8(3):e59896. Epub 2013/03/29. doi: [10.1371/journal.pone.0059896](https://doi.org/10.1371/journal.pone.0059896) PMID: [23536892](https://pubmed.ncbi.nlm.nih.gov/23536892/); PubMed Central PMCID: PMC3607558.

41. Kremlev SG, Umstead TM, Phelps DS. Surfactant protein A regulates cytokine production in the monocytic cell line THP-1. *Am J Physiol*. 1997; 272(5 Pt 1):L996–1004. PMID: [9176266](#).
42. Kremlev SG, Phelps DS. Effect of SP-A and surfactant lipids on expression of cell surface markers in the THP-1 monocytic cell line. *Am J Physiol*. 1997; 272(6 Pt 1):L1070–7. PMID: [9227506](#).
43. Koptides M, Umstead TM, Floros J, Phelps DS. Surfactant protein A activates NF-kappa B in the THP-1 monocytic cell line. *Am J Physiol*. 1997; 273(2 Pt 1):L382–8. Epub 1997/08/01. PMID: [9277450](#).
44. Phelps DS, Umstead TM, Quintero OA, Yengo CM, Floros J. In vivo rescue of alveolar macrophages from SP-A knockout mice with exogenous SP-A nearly restores a wild type intracellular proteome; actin involvement. *Proteome science*. 2011; 9:67. Epub 2011/11/01. doi: [10.1186/1477-5956-9-67](#) PMID: [22035134](#); PubMed Central PMCID: PMC3219558.
45. LeVine AM, Kurak KE, Wright JR, Watford WT, Bruno MD, Ross GF, et al. Surfactant protein-A binds group B streptococcus enhancing phagocytosis and clearance from lungs of surfactant protein-A-deficient mice. *Am J Respir Cell Mol Biol*. 1999; 20(2):279–86. Epub 1999/01/28. PMID: [9922219](#).
46. Song M, Phelps DS. Comparison of SP-A and LPS effects on the THP-1 monocytic cell line. *Am J Physiol Lung Cell Mol Physiol*. 2000; 279(1):L110–7. PMID: [10893209](#).
47. Song M, Phelps DS. Interaction of surfactant protein A with lipopolysaccharide and regulation of inflammatory cytokines in the THP-1 monocytic cell line. *Infect Immun*. 2000; 68(12):6611–7. PMID: [11083772](#).
48. Agrawal V, Smart K, Jilling T, Hirsch E. Surfactant protein (SP)-A suppresses preterm delivery and inflammation via TLR2. *PLoS One*. 2013; 8(5):e63990. doi: [10.1371/journal.pone.0063990](#) PMID: [23700442](#); PubMed Central PMCID: PMC3659120.
49. Foley JP, Lam D, Jiang H, Liao J, Cheong N, McDevitt TM, et al. Toll-like receptor 2 (TLR2), transforming growth factor-beta, hyaluronan (HA), and receptor for HA-mediated motility (RHAMM) are required for surfactant protein A-stimulated macrophage chemotaxis. *J Biol Chem*. 2012; 287(44):37406–19. doi: [10.1074/jbc.M112.360982](#) PMID: [22948158](#); PubMed Central PMCID: PMC3481337.
50. Montalbano AP, Hawgood S, Mendelson CR. Mice deficient in surfactant protein A (SP-A) and SP-D or in TLR2 manifest delayed parturition and decreased expression of inflammatory and contractile genes. *Endocrinology*. 2013; 154(1):483–98. Epub 2012/11/28. doi: [10.1210/en.2012-1797](#) PMID: [23183169](#); PubMed Central PMCID: PMC3529364.
51. Wang G, Phelps DS, Umstead TM, Floros J. Human SP-A protein variants derived from one or both genes stimulate TNF-alpha production in the THP-1 cell line. *Am J Physiol Lung Cell Mol Physiol*. 2000; 278(5):L946–54. Epub 2000/04/27. PMID: [10781424](#).
52. Brendle SA, Culp TD, Broutian TR, Christensen ND. Binding and neutralization characteristics of a panel of monoclonal antibodies to human papillomavirus 58. *J Gen Virol*. 2010; 91(Pt 7):1834–9. doi: [10.1099/vir.0.017228-0](#) PMID: [20181746](#); PubMed Central PMCID: PMC3052528.
53. Clark JC, Wert SE, Bachurski CJ, Stahlman MT, Stripp BR, Weaver TE, et al. Targeted disruption of the surfactant protein B gene disrupts surfactant homeostasis, causing respiratory failure in newborn mice. *Proc Natl Acad Sci U S A*. 1995; 92(17):7794–8. Epub 1995/08/15. PMID: [7644495](#).
54. Li G, Siddiqui J, Hendry M, Akiyama J, Edmondson J, Brown C, et al. Surfactant protein-A—deficient mice display an exaggerated early inflammatory response to a beta-resistant strain of influenza A virus. *Am J Respir Cell Mol Biol*. 2002; 26(3):277–82. Epub 2002/02/28. PMID: [11867335](#).
55. Hawgood S, Ochs M, Jung A, Akiyama J, Allen L, Brown C, et al. Sequential targeted deficiency of SP-A and-D leads to progressive alveolar lipoproteinosis and emphysema. *Am J Physiol Lung Cell Mol Physiol*. 2002; 283(5):L1002–10. doi: [10.1152/ajplung.00118.2002](#) PMID: [12376353](#).
56. Booth JL, Umstead TM, Hu S, Dybvig KF, Cooper TK, Wilson RP, et al. Housing Conditions Modulate the Severity of Mycoplasma pulmonis Infection in Mice Deficient in Class A Scavenger Receptor. *Comparative medicine*. 2014; 64(6):424–39. PMID: [25527023](#); PubMed Central PMCID: PMC4275078.
57. Huang W, Wang G, Phelps DS, Al-Mondhiry H, Floros J. Combined SP-A-bleomycin effect on cytokines by THP-1 cells: impact of surfactant lipids on this effect. *Am J Physiol Lung Cell Mol Physiol*. 2002; 283(1):L94–L102. doi: [10.1152/ajplung.00434.2001](#) PMID: [12060565](#).
58. Haagsman HP, Hawgood S, Sargeant T, Buckley D, White RT, Drickamer K, et al. The major lung surfactant protein, SP 28–36, is a calcium-dependent, carbohydrate-binding protein. *J Biol Chem*. 1987; 262(29):13877–80. PMID: [2820982](#).
59. Rabilloud T, Brodard V, Peltre G, Righetti PG, Ettori C. Modified silver staining for immobilized pH gradients. *Electrophoresis*. 1992; 13(4):264–6. PMID: [1628608](#).
60. Bustin SA, Benes V, Garson JA, Hellemans J, Huggett J, Kubista M, et al. The MIQE guidelines: minimum information for publication of quantitative real-time PCR experiments. *Clin Chem*. 2009; 55(4):611–22. Epub 2009/02/28. doi: [10.1373/clinchem.2008.112797](#) PMID: [19246619](#).

61. Korfhagen TR, Bruno MD, Ross GF, Huelsman KM, Ikegami M, Jobe AH, et al. Altered surfactant function and structure in SP-A gene targeted mice. *Proc Natl Acad Sci U S A*. 1996; 93(18):9594–9. PMID: [8790375](#).
62. Wu H, Kuzmenko A, Wan S, Schaffer L, Weiss A, Fisher JH, et al. Surfactant proteins A and D inhibit the growth of Gram-negative bacteria by increasing membrane permeability. *J Clin Invest*. 2003; 111(10):1589–602. PMID: [12750409](#).
63. Mikerov AN, Haque R, Gan X, Guo X, Phelps DS, Floros J. Ablation of SP-A has a negative impact on the susceptibility of mice to *Klebsiella pneumoniae* infection after ozone exposure: sex differences. *Respir Res*. 2008; 9:77. Epub 2008/12/06. doi: [10.1186/1465-9921-9-77](#) PMID: [19055785](#); PubMed Central PMCID: PMC2655296.
64. Haque R, Umstead TM, Ponnuru P, Guo X, Hawgood S, Phelps DS, et al. Role of surfactant protein-A (SP-A) in lung injury in response to acute ozone exposure of SP-A deficient mice. *Toxicol Appl Pharmacol*. 2007; 220(1):72–82. doi: [10.1016/j.taap.2006.12.017](#) PMID: [17307210](#); PubMed Central PMCID: PMC1906716.
65. Ostuni R, Zanoni I, Granucci F. Deciphering the complexity of Toll-like receptor signaling. *Cell Mol Life Sci*. 2010; 67(24):4109–34. Epub 2010/08/04. doi: [10.1007/s00018-010-0464-x](#) PMID: [20680392](#).
66. Zanoni I, Ostuni R, Marek LR, Barresi S, Barbalat R, Barton GM, et al. CD14 controls the LPS-induced endocytosis of Toll-like receptor 4. *Cell*. 2011; 147(4):868–80. doi: [10.1016/j.cell.2011.09.051](#) PMID: [22078883](#); PubMed Central PMCID: PMC3217211.
67. Hayden MS, Ghosh S. NF-kappaB, the first quarter-century: remarkable progress and outstanding questions. *Genes & development*. 2012; 26(3):203–34. doi: [10.1101/gad.183434.111](#) PMID: [22302935](#); PubMed Central PMCID: PMC3278889.
68. Poussin C, Foti M, Carpentier JL, Pugin J. CD14-dependent endotoxin internalization via a macropinocytotic pathway. *J Biol Chem*. 1998; 273(32):20285–91. PMID: [9685378](#).
69. Macia E, Ehrlich M, Massol R, Boucrot E, Brunner C, Kirchhausen T. Dynasore, a cell-permeable inhibitor of dynamin. *Developmental cell*. 2006; 10(6):839–50. doi: [10.1016/j.devcel.2006.04.002](#) PMID: [16740485](#).
70. Park RJ, Shen H, Liu L, Liu X, Ferguson SM, De Camilli P. Dynamin triple knockout cells reveal off target effects of commonly used dynamin inhibitors. *J Cell Sci*. 2013; 126(Pt 22):5305–12. doi: [10.1242/jcs.138578](#) PMID: [24046449](#); PubMed Central PMCID: PMC3828596.
71. Mesaki K, Tanabe K, Obayashi M, Oe N, Takei K. Fission of tubular endosomes triggers endosomal acidification and movement. *PLoS One*. 2011; 6(5):e19764. doi: [10.1371/journal.pone.0019764](#) PMID: [21572956](#); PubMed Central PMCID: PMC3091875.
72. Kockx M, Karunakaran D, Traini M, Xue J, Huang KY, Nawara D, et al. Pharmacological inhibition of dynamin II reduces constitutive protein secretion from primary human macrophages. *PLoS One*. 2014; 9(10):e111186. doi: [10.1371/journal.pone.0111186](#) PMID: [25347775](#); PubMed Central PMCID: PMC4210248.
73. Kagan JC, Su T, Horng T, Chow A, Akira S, Medzhitov R. TRAM couples endocytosis of Toll-like receptor 4 to the induction of interferon-beta. *Nat Immunol*. 2008; 9(4):361–8. doi: [10.1038/ni1569](#) PMID: [18297073](#); PubMed Central PMCID: PMC4112825.
74. Koivusalo M, Welch C, Hayashi H, Scott CC, Kim M, Alexander T, et al. Amiloride inhibits macropinocytosis by lowering submembranous pH and preventing Rac1 and Cdc42 signaling. *J Cell Biol*. 2010; 188(4):547–63. doi: [10.1083/jcb.200908086](#) PMID: [20156964](#); PubMed Central PMCID: PMC2828922.
75. Yoshida S, Hoppe AD, Araki N, Swanson JA. Sequential signaling in plasma-membrane domains during macropinosome formation in macrophages. *J Cell Sci*. 2009; 122(Pt 18):3250–61. doi: [10.1242/jcs.053207](#) PMID: [19690049](#); PubMed Central PMCID: PMC2736863.
76. Fujii M, Kawai K, Egami Y, Araki N. Dissecting the roles of Rac1 activation and deactivation in macropinocytosis using microscopic photo-manipulation. *Scientific reports*. 2013; 3:2385. doi: [10.1038/srep02385](#) PMID: [23924974](#); PubMed Central PMCID: PMC3737501.
77. Huang W, Wang G, Phelps DS, Al-Mondhry H, Floros J. Human SP-A genetic variants and bleomycin-induced cytokine production by THP-1 cells: effect of ozone-induced SP-A oxidation. *Am J Physiol Lung Cell Mol Physiol*. 2004; 286(3):L546–53. doi: [10.1152/ajplung.00267.2003](#) PMID: [14617519](#).
78. Phelps DS, Smith LM, Taeusch HW. Characterization and partial amino acid sequence of a low molecular weight surfactant protein. *Am Rev Respir Dis*. 1987; 135(5):1112–7. PMID: [3579010](#).
79. Holmskov U, Mollenhauer J, Madsen J, Vitved L, Gronlund J, Tornoe I, et al. Cloning of gp-340, a putative opsonin receptor for lung surfactant protein D. *Proc Natl Acad Sci U S A*. 1999; 96(19):10794–9. PMID: [10485905](#); PubMed Central PMCID: PMC17962.
80. Fan Y, Zhang J, Cai L, Wang S, Liu C, Zhang Y, et al. The effect of anti-inflammatory properties of ferritin light chain on lipopolysaccharide-induced inflammatory response in murine macrophages. *Biochim Biophys Acta*. 2014; 1843(11):2775–83. doi: [10.1016/j.bbamcr.2014.06.015](#) PMID: [24983770](#).

81. Ueno T, Linder S, Na CL, Rice WR, Johansson J, Weaver TE. Processing of pulmonary surfactant protein B by napsin and cathepsin H. *J Biol Chem*. 2004; 279(16):16178–84. doi: [10.1074/jbc.M312029200](https://doi.org/10.1074/jbc.M312029200) PMID: [14766755](https://pubmed.ncbi.nlm.nih.gov/14766755/).
82. Woischnik M, Bauer A, Aboutaam R, Pamir A, Stanzel F, de Blic J, et al. Cathepsin H and napsin A are active in the alveoli and increased in alveolar proteinosis. *Eur Respir J*. 2008; 31(6):1197–204. doi: [10.1183/09031936.00081207](https://doi.org/10.1183/09031936.00081207) PMID: [18216060](https://pubmed.ncbi.nlm.nih.gov/18216060/).
83. Jakel A, Qaseem AS, Kishore U, Sim RB. Ligands and receptors of lung surfactant proteins SP-A and SP-D. *Frontiers in bioscience*. 2013; 18:1129–40. PMID: [23747872](https://pubmed.ncbi.nlm.nih.gov/23747872/).
84. Kitchens RL, Munford RS. CD14-dependent internalization of bacterial lipopolysaccharide (LPS) is strongly influenced by LPS aggregation but not by cellular responses to LPS. *J Immunol*. 1998; 160(4):1920–8. PMID: [9469454](https://pubmed.ncbi.nlm.nih.gov/9469454/).
85. Gegner JA, Ulevitch RJ, Tobias PS. Lipopolysaccharide (LPS) signal transduction and clearance. Dual roles for LPS binding protein and membrane CD14. *J Biol Chem*. 1995; 270(10):5320–5. PMID: [7534294](https://pubmed.ncbi.nlm.nih.gov/7534294/).
86. Jiang Z, Georgel P, Du X, Shamel L, Sovath S, Mudd S, et al. CD14 is required for MyD88-independent LPS signaling. *Nat Immunol*. 2005; 6(6):565–70. Epub 2005/05/17. doi: [10.1038/ni1207](https://doi.org/10.1038/ni1207) PMID: [15895089](https://pubmed.ncbi.nlm.nih.gov/15895089/).
87. Dunzendorfer S, Lee HK, Soldau K, Tobias PS. TLR4 is the signaling but not the lipopolysaccharide uptake receptor. *J Immunol*. 2004; 173(2):1166–70. PMID: [15240706](https://pubmed.ncbi.nlm.nih.gov/15240706/).
88. Zivkovic A, Sharif O, Stich K, Doninger B, Biaggio M, Colinge J, et al. TLR 2 and CD14 mediate innate immunity and lung inflammation to staphylococcal Panton-Valentine leukocidin in vivo. *J Immunol*. 2011; 186(3):1608–17. Epub 2010/12/24. doi: [10.4049/jimmunol.1001665](https://doi.org/10.4049/jimmunol.1001665) PMID: [21178007](https://pubmed.ncbi.nlm.nih.gov/21178007/).
89. Jozefowski S, Biedron R, Srottek M, Chadzinska M, Marcinkiewicz J. The class A scavenger receptor SR-A/CD204 and the class B scavenger receptor CD36 regulate immune functions of macrophages differently. *Innate Immun*. 2014; 20(8):826–47. doi: [10.1177/1753425913510960](https://doi.org/10.1177/1753425913510960) PMID: [24257313](https://pubmed.ncbi.nlm.nih.gov/24257313/).
90. Czerkies M, Borzecka K, Zdioruk MI, Plociennikowska A, Sobota A, Kwiatkowska K. An interplay between scavenger receptor A and CD14 during activation of J774 cells by high concentrations of LPS. *Immunobiology*. 2013. doi: [10.1016/j.imbio.2013.04.005](https://doi.org/10.1016/j.imbio.2013.04.005) PMID: [23669238](https://pubmed.ncbi.nlm.nih.gov/23669238/).
91. Yu H, Ha T, Liu L, Wang X, Gao M, Kelley J, et al. Scavenger receptor A (SR-A) is required for LPS-induced TLR4 mediated NF-kappaB activation in macrophages. *Biochim Biophys Acta*. 2012; 1823(7):1192–8. doi: [10.1016/j.bbamcr.2012.05.004](https://doi.org/10.1016/j.bbamcr.2012.05.004) PMID: [22627090](https://pubmed.ncbi.nlm.nih.gov/22627090/); PubMed Central PMCID: [PMC3382073](https://pubmed.ncbi.nlm.nih.gov/PMC3382073/).
92. Perera PY, Mayadas TN, Takeuchi O, Akira S, Zaks-Zilberman M, Goyert SM, et al. CD11b/CD18 acts in concert with CD14 and Toll-like receptor (TLR) 4 to elicit full lipopolysaccharide and taxol-inducible gene expression. *J Immunol*. 2001; 166(1):574–81. PMID: [11123339](https://pubmed.ncbi.nlm.nih.gov/11123339/).
93. Hawley KL, Martin-Ruiz I, Iglesias-Pedraz JM, Berwin B, Anguita J. CD14 targets complement receptor 3 to lipid rafts during phagocytosis of *Borrelia burgdorferi*. *International journal of biological sciences*. 2013; 9(8):803–10. doi: [10.7150/ijbs.7136](https://doi.org/10.7150/ijbs.7136) PMID: [23983613](https://pubmed.ncbi.nlm.nih.gov/23983613/); PubMed Central PMCID: [PMC3753444](https://pubmed.ncbi.nlm.nih.gov/PMC3753444/).
94. Tanimura N, Saitoh S, Matsumoto F, Akashi-Takamura S, Miyake K. Roles for LPS-dependent interaction and relocation of TLR4 and TRAM in TRIF-signaling. *Biochem Biophys Res Commun*. 2008; 368(1):94–9. doi: [10.1016/j.bbrc.2008.01.061](https://doi.org/10.1016/j.bbrc.2008.01.061) PMID: [18222170](https://pubmed.ncbi.nlm.nih.gov/18222170/).
95. Husebye H, Halaas O, Stenmark H, Tunheim G, Sandanger O, Bogen B, et al. Endocytic pathways regulate Toll-like receptor 4 signaling and link innate and adaptive immunity. *EMBO J*. 2006; 25(4):683–92. doi: [10.1038/sj.emboj.7600991](https://doi.org/10.1038/sj.emboj.7600991) PMID: [16467847](https://pubmed.ncbi.nlm.nih.gov/16467847/); PubMed Central PMCID: [PMC1383569](https://pubmed.ncbi.nlm.nih.gov/PMC1383569/).
96. Kim KS, Kim JS, Park JY, Suh YH, Jou I, Joe EH, et al. DJ-1 associates with lipid rafts by palmitoylation and regulates lipid rafts-dependent endocytosis in astrocytes. *Hum Mol Genet*. 2013; 22(23):4805–17. doi: [10.1093/hmg/ddt332](https://doi.org/10.1093/hmg/ddt332) PMID: [23847046](https://pubmed.ncbi.nlm.nih.gov/23847046/).
97. Brandt KJ, Fickentscher C, Kruihof EK, de Moerloose P. TLR2 ligands induce NF-kappaB activation from endosomal compartments of human monocytes. *PLoS One*. 2013; 8(12):e80743. doi: [10.1371/journal.pone.0080743](https://doi.org/10.1371/journal.pone.0080743) PMID: [24349012](https://pubmed.ncbi.nlm.nih.gov/24349012/); PubMed Central PMCID: [PMC3861177](https://pubmed.ncbi.nlm.nih.gov/PMC3861177/).
98. Shamsul HM, Hasebe A, Iyori M, Ohtani M, Kiura K, Zhang D, et al. The Toll-like receptor 2 (TLR2) ligand FSL-1 is internalized via the clathrin-dependent endocytic pathway triggered by CD14 and CD36 but not by TLR2. *Immunology*. 2010; 130(2):262–72. doi: [10.1111/j.1365-2567.2009.03232.x](https://doi.org/10.1111/j.1365-2567.2009.03232.x) PMID: [20113368](https://pubmed.ncbi.nlm.nih.gov/20113368/); PubMed Central PMCID: [PMC2878470](https://pubmed.ncbi.nlm.nih.gov/PMC2878470/).
99. Plociennikowska A, Hromada-Judycka A, Borzecka K, Kwiatkowska K. Co-operation of TLR4 and raft proteins in LPS-induced pro-inflammatory signaling. *Cell Mol Life Sci*. 2015; 72(3):557–81. doi: [10.1007/s00018-014-1762-5](https://doi.org/10.1007/s00018-014-1762-5) PMID: [25332099](https://pubmed.ncbi.nlm.nih.gov/25332099/); PubMed Central PMCID: [PMC4293489](https://pubmed.ncbi.nlm.nih.gov/PMC4293489/).

100. Hall A. Ras-related GTPases and the cytoskeleton. *Mol Biol Cell*. 1992; 3(5):475–9. PMID: [1611153](#); PubMed Central PMCID: PMC275601.
101. Egami Y, Taguchi T, Maekawa M, Arai H, Araki N. Small GTPases and phosphoinositides in the regulatory mechanisms of macropinosome formation and maturation. *Frontiers in physiology*. 2014; 5:374. doi: [10.3389/fphys.2014.00374](#) PMID: [25324782](#); PubMed Central PMCID: PMC4179697.
102. Tong L, Tergaonkar V. Rho protein GTPases and their interactions with NFkappaB: crossroads of inflammation and matrix biology. *Bioscience reports*. 2014; 34(3). doi: [10.1042/BSR20140021](#) PMID: [24877606](#); PubMed Central PMCID: PMC4069681.
103. Hsu HY, Chiu SL, Wen MH, Chen KY, Hua KF. Ligands of macrophage scavenger receptor induce cytokine expression via differential modulation of protein kinase signaling pathways. *J Biol Chem*. 2001; 276(31):28719–30. doi: [10.1074/jbc.M011117200](#) PMID: [11390374](#).
104. Hoogerwerf JJ, de Vos AF, van't Veer C, Bresser P, de Boer A, Tanck MW, et al. Priming of alveolar macrophages upon instillation of lipopolysaccharide in the human lung. *Am J Respir Cell Mol Biol*. 2010; 42(3):349–56. Epub 2009/05/19. doi: [10.1165/rcmb.2008-0362OC](#) PMID: [19448156](#).
105. Philippart F, Fitting C, Cavaillon JM. Lung microenvironment contributes to the resistance of alveolar macrophages to develop tolerance to endotoxin*. *Crit Care Med*. 2012; 40(11):2987–96. doi: [10.1097/CCM.0b013e31825b8d57](#) PMID: [22878679](#).
106. Tomlinson GS, Booth H, Petit SJ, Potton E, Towers GJ, Miller RF, et al. Adherent human alveolar macrophages exhibit a transient pro-inflammatory profile that confounds responses to innate immune stimulation. *PLoS One*. 2012; 7(6):e40348. Epub 2012/07/07. doi: [10.1371/journal.pone.0040348](#) PMID: [22768282](#); PubMed Central PMCID: PMC3386998.
107. Islam MA, Proll M, Holker M, Tholen E, Tesfaye D, Looft C, et al. Alveolar macrophage phagocytic activity is enhanced with LPS priming, and combined stimulation of LPS and lipoteichoic acid synergistically induce pro-inflammatory cytokines in pigs. *Innate Immun*. 2013. doi: [10.1177/1753425913477166](#) PMID: [23608822](#).
108. Kasahara K, Matsumura Y, Ui K, Kasahara K, Komatsu Y, Mikasa K, et al. Intranasal priming of newborn mice with microbial extracts increases opsonic factors and mature CD11c+ cells in the airway. *Am J Physiol Lung Cell Mol Physiol*. 2012; 303(9):L834–43. doi: [10.1152/ajplung.00031.2012](#) PMID: [22923643](#).
109. Hawgood S, Benson BJ, Hamilton RL Jr. Effects of a surfactant-associated protein and calcium ions on the structure and surface activity of lung surfactant lipids. *Biochemistry*. 1985; 24(1):184–90. Epub 1985/01/01. PMID: [3922400](#).
110. Glasser SW, Maxfield MD, Ruetschilling TL, Akinbi HT, Baatz JE, Kitzmiller JA, et al. Persistence of LPS Induced Lung Inflammation in Surfactant Protein-C Deficient Mice. *Am J Respir Cell Mol Biol*. 2013. doi: [10.1165/rcmb.2012-0374OC](#) PMID: [23795648](#).
111. Abate W, Alghaithy AA, Parton J, Jones KP, Jackson SK. Surfactant lipids regulate LPS-induced interleukin-8 production in A549 lung epithelial cells by inhibiting translocation of TLR4 into lipid raft domains. *Journal of lipid research*. 2009. Epub 2009/08/04. doi: [jlr.M000513](#) [pii]doi: [10.1194/jlr.M000513](#) PMID: [19648651](#).
112. Tonks A, Parton J, Tonks AJ, Morris RH, Finall A, Jones KP, et al. Surfactant phospholipid DPPC down-regulates monocyte respiratory burst via modulation of PKC. *Am J Physiol Lung Cell Mol Physiol*. 2005; 288(6):L1070–80. Epub 2005/02/01. doi: [00386.2004](#) [pii] doi: [10.1152/ajplung.00386.2004](#) PMID: [15681395](#).
113. Raychaudhuri B, Abraham S, Bonfield TL, Malur A, Deb A, DiDonato JA, et al. Surfactant blocks lipopolysaccharide signaling by inhibiting both mitogen-activated protein and I kappa B kinases in human alveolar macrophages. *Am J Respir Cell Mol Biol*. 2004; 30(2):228–32. Epub 2003/08/16. doi: [10.1165/rcmb.2003-0263OC](#) 2003-0263OC [pii]. PMID: [12920056](#).
114. Golioto A, Wright JR. Effects of surfactant lipids and surfactant protein a on host defense functions of rat alveolar macrophages. *Pediatr Res*. 2002; 51(2):220–7. Epub 2002/01/26. PMID: [11809918](#).
115. Vazquez de Lara L, Becerril C, Montano M, Ramos C, Maldonado V, Melendez J, et al. Surfactant components modulate fibroblast apoptosis and type I collagen and collagenase-1 expression. *Am J Physiol Lung Cell Mol Physiol*. 2000; 279(5):L950–7. PMID: [11053032](#).
116. Miles PR, Bowman L, Rao KM, Baatz JE, Huffman L. Pulmonary surfactant inhibits LPS-induced nitric oxide production by alveolar macrophages. *Am J Physiol*. 1999; 276(1 Pt 1):L186–96. Epub 1999/01/14. PMID: [9887071](#).
117. Antal JM, Divis LT, Erzurum SC, Wiedemann HP, Thomassen MJ. Surfactant suppresses NF-kappa B activation in human monocytic cells. *Am J Respir Cell Mol Biol*. 1996; 14(4):374–9. Epub 1996/04/01. PMID: [8600942](#).

118. Augusto L, Le Blay K, Auger G, Blanot D, Chaby R. Interaction of bacterial lipopolysaccharide with mouse surfactant protein C inserted into lipid vesicles. *Am J Physiol Lung Cell Mol Physiol*. 2001; 281(4):L776–85. Epub 2001/09/15. PMID: [11557581](#).
119. Glasser SW, Witt TL, Senft AP, Baatz JE, Folger D, Maxfield MD, et al. Surfactant protein C-deficient mice are susceptible to respiratory syncytial virus infection. *Am J Physiol Lung Cell Mol Physiol*. 2009; 297(1):L64–72. doi: [10.1152/ajplung.90640.2008](#) PMID: [19304906](#); PubMed Central PMCID: PMC2711816.
120. Kuronuma K, Mitsuzawa H, Takeda K, Nishitani C, Chan ED, Kuroki Y, et al. Anionic Pulmonary Surfactant Phospholipids Inhibit inflammatory responses from Alveolar Macrophages and U937 Cells by Binding the Lipopolysaccharide Interacting Proteins CD14 and MD2. *J Biol Chem*. 2009. Epub 2009/07/09. doi: M109.040832 [pii] doi: [10.1074/jbc.M109.040832](#) PMID: [19584052](#).
121. Yang S, Milla C, Panoskaltis-Mortari A, Hawgood S, Blazar BR, Haddad IY. Surfactant protein A decreases lung injury and mortality after murine marrow transplantation. *Am J Respir Cell Mol Biol*. 2002; 27(3):297–305. PMID: [12204891](#).